Thin Film Growth of Topological Insulators Bi_2Se_3 and $(Bi,Sb)_2Te_3$ toward Bulk-insulating Features and Enhanced Interfacial Exchange Coupling on Rare Earth Iron Garnets

Chun-Chia Chen (陳俊嘉)

Department of Physics, National Tsing-Hua University, Taiwan

Advisor: J. Raynien Kwo (郭瑞年)

Department of Physics, National Tsing-Hua University, Taiwan

Advisor: Minghwei Hong (洪銘輝)

Department of Physics, National Taiwan University, Taiwan

Acknowledgement

- **MBE**

  C. C. Chen and K. H. M. Chen

- **Sputtering**

  C. C. Tseng, M. X. Guo, and Dr. C. N. Wu

- **XRD**

  C. K. Cheng

- **TEM**

  Dr. C. T. Wu

- **Transport**

  S. R. Yang, J. S. Wei, Y. T. Fanchiang, and W. J. Zou

- **XPS**

  S. W. Huang and K. Y. Lin

- **ARPES**

  S. W. Huang and K. Y. Lin

- **FMR**

  Y. T. Fanchiang

- **Spin pumping**

  Y. T. Fanchiang

- **Discussion & suggestion**

  Dr. C. N. Wu, Dr. Y. K. Liu, and Y. H. Lin

Outline

- **Introduction**
  - 3D topological insulators (TIs)
  - Breaking time reversal symmetry by magnetic proximity effect (MPE)
    - Demand for a reproducible growth method
  - Manipulating the Fermi level (E_F) toward the Dirac point
  - Motivation
- **Bi_2Se_3 / Rare earth iron garnet (ReIG)**
  - Advantage of ReIGs
    - Yttrium iron garnet (YIG) & thulium iron garnet (TmIG)
  - Growth method: Se-buffered low-temperature (SBLT) growth
  - Improvement in crystallinities (vs. conventional two-step growth)
  - Enhancement of interfacial exchange coupling
    - Observation of anomalous Hall effect (AHE)
    - Large negative shift in H_{res} probed by ferromagnetic resonance (FMR)

Outline

- **Introduction**
  - 3D topological insulators (TIs)
  - Breaking time reversal symmetry by magnetic proximity effect (MPE)
    - Demand for a reproducible growth method
  - Manipulating the Fermi level (E_F) toward the Dirac point
  - Motivation

- **Bi_2Se_3 / Rare earth iron garnet (ReIG)**
  - Advantage of ReIGs
    - Yttrium iron garnet (YIG) & thulium iron garnet (TmIG)
  - Growth method: Se-buffered low-temperature (SBLT) growth
  - Improvement in crystallinities (vs. conventional two-step growth)
  - Enhancement of interfacial exchange coupling
    - Observation of anomalous Hall effect (AHE)
    - Large negative shift in H_{res} probed by ferromagnetic resonance (FMR)

Outline

- **$(Bi,Sb)_2Te_3$ / α-Al_2O_3 & $(Bi,Sb)_2Te_3$ / TmIG**
  - Characterization of structural properties
    - Higher-temperature growth of Sb_2Te_3 & $(Bi,Sb)_2Te_3$
  - Evidences of manipulating E_F toward bulk-insulating features
    - Detection of two conductive transport channels
    - Band structure engineering revealed by ARPES
  - Electronic transport & magnetoresistance analysis
    - Observation of room-temperature AHE

- **Conclusion**

3D topological insulators (TIs)

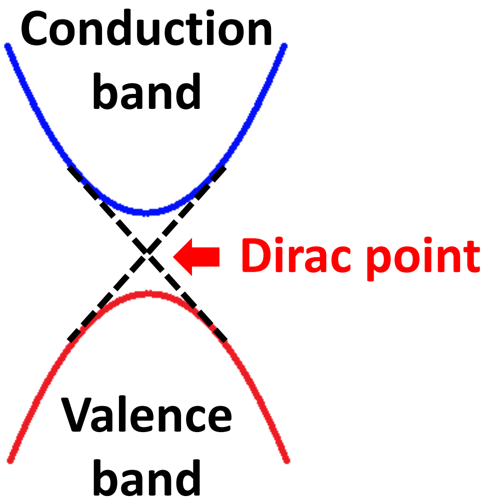

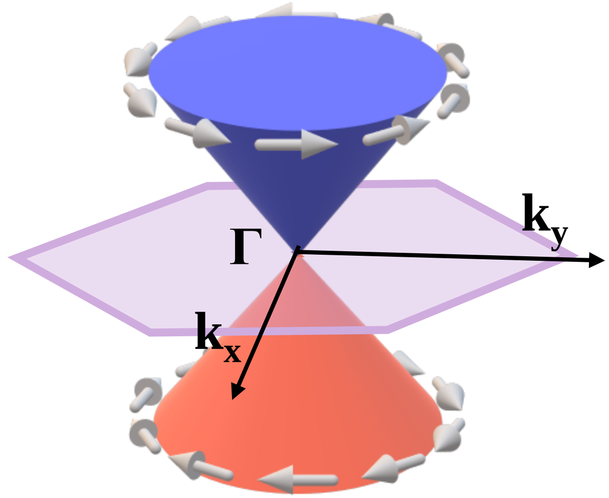

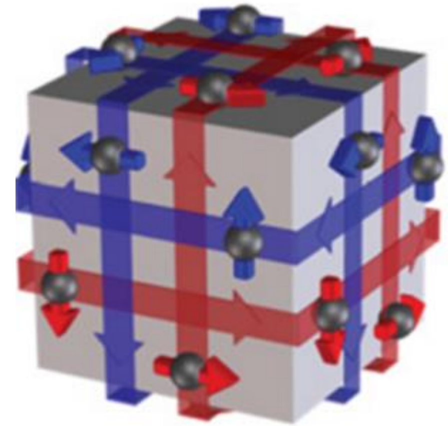

- 3D TIs: Bi_2Se_3, Bi_2Te_3, and Sb_2Te_3
- Band inversion induced by strong SOC
- Protected by time-reversal symmetry

- Topological surface states (TSSs)
  - Spin-momentum locking
  - Massless Dirac fermion
- More…
  - High spin-to-charge conversion
  - Weak anti-localization (WAL) effect
  - Forbidden-back-scattering transport

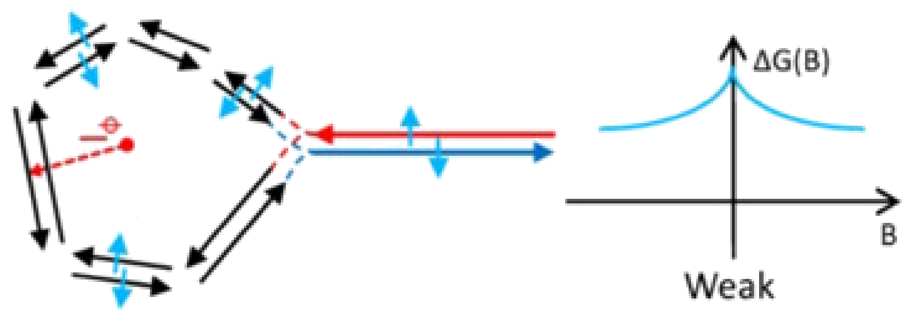

Spin-momentum locked

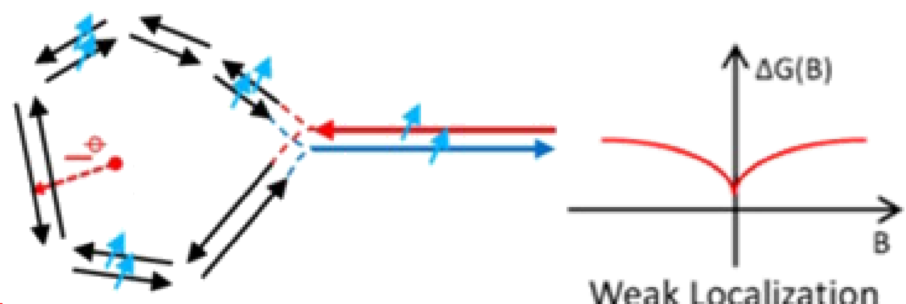

No Spin-momentum locking

M. Brahlek *et al.*, Solid State Commun. **215-216**, 54-62 (2015).

Breaking TRS by MPE

Breaking Time Reversal Symmetry (TRS) in TIs

➡ Quantum anomalous Hall effect (QAHE)

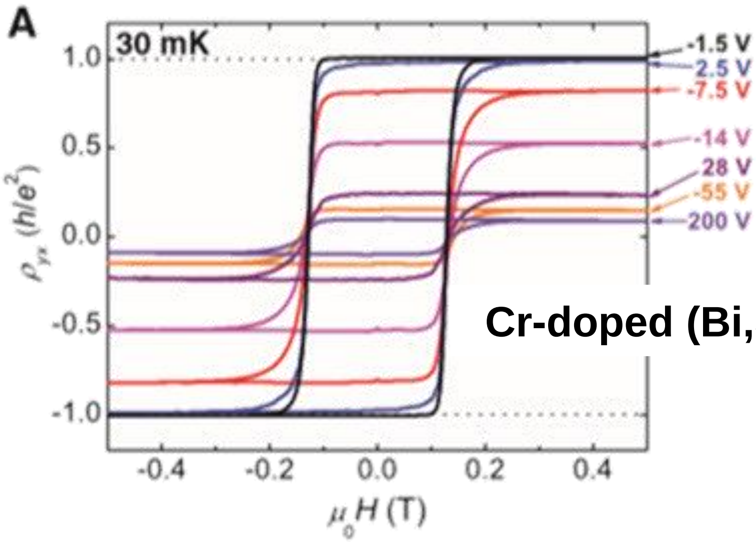

Cr-doped $(Bi,Sb)_2Te_3$

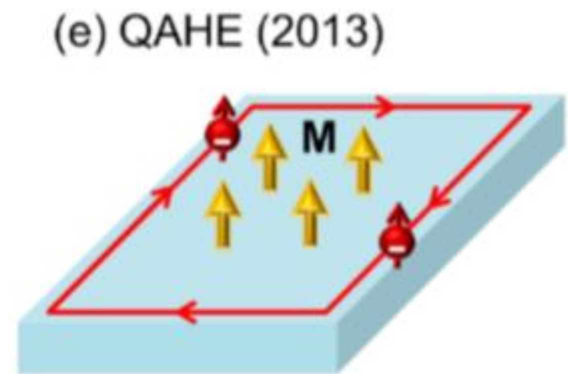

C.-Z. Chang *et al*., Science **340**(6129), 167-170 (2013).

C.-Z. Chang *et al*., *Nat. Mater.* **14**, 473–477 (2015).

C.-Z. Chang *et al*., J. Phys.: Condens. Matter **28,** 123002 (2016).

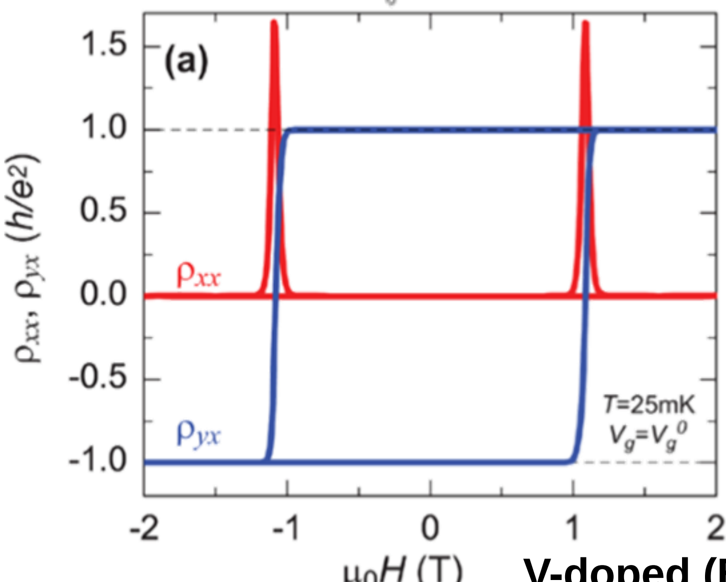

V-doped $(Bi,Sb)_2Te_3$

Features

- **Quantized plateau ($\frac{h}{e^2}$) in ρ_{xy}**
- **Approaching zero resistivity in ρ_{xx}**
- **Dissipationless transport**

Breaking TRS by MPE

Breaking Time Reversal Symmetry (TRS) in TIs

➡ **Quantum anomalous Hall effect (QAHE)**

Ways to break TRS in TIs:
Introducing magnetic moments

- **Transition metal doping**
- **Magnetic proximity effect (MPE)**

Magnetic proximity effect

Advantages of MPE:

- **Higher T_C than that of magnetic doping**
- **No crystal defects**
- **Uniform magnetization**

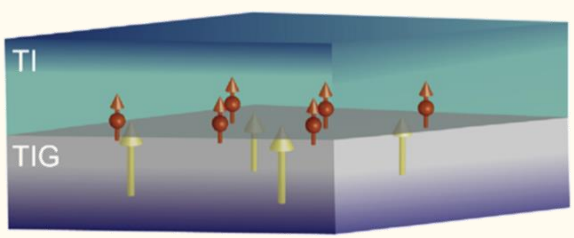

C. Tang *et al.*, Sci. Adv. **3** (6), e1700307 (2017).

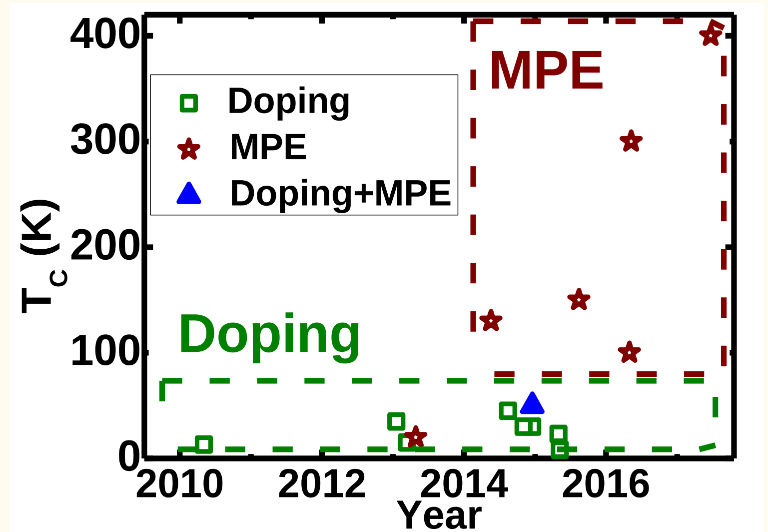

$$E = \pm\sqrt{\left(\hbar v_F k_x + \frac{J}{2}M_y\right)^2 + \left(\hbar v_F k_y - \frac{J}{2}M_x\right)^2 + \left(\frac{J}{2}M_z\right)^2}$$

H. Z. Lu *et al.*, Phys. Rev. Lett. **107**, 076801 (2011).

Breaking TRS by MPE

Breaking Time Reversal Symmetry (TRS) in TIs

➡ **Quantum anomalous Hall effect (QAHE)**

Ways to break TRS in TIs:
Introducing magnetic moments

→ **Transition metal doping**

→ **Magnetic proximity effect (MPE)**

Magnetic proximity effect

Advantages of MPE:

- **Higher T_C than that of magnetic doping**
- **No crystal defects**
- **Uniform magnetization**

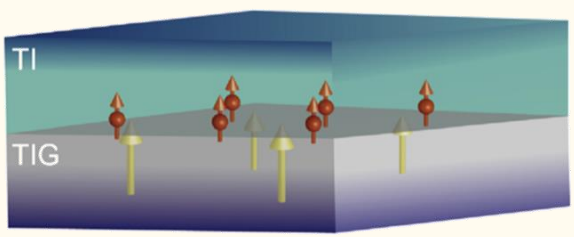

C. Tang *et al.*, Sci. Adv. **3** (6), e1700307 (2017).

TI/MI hetero-structure with a very small lattice mismatch

- **Persistence of MPE to room temperature**
- **Low T_C (~17 K)**
- **In-plane magnetic anisotropy (IMA) of EuS**

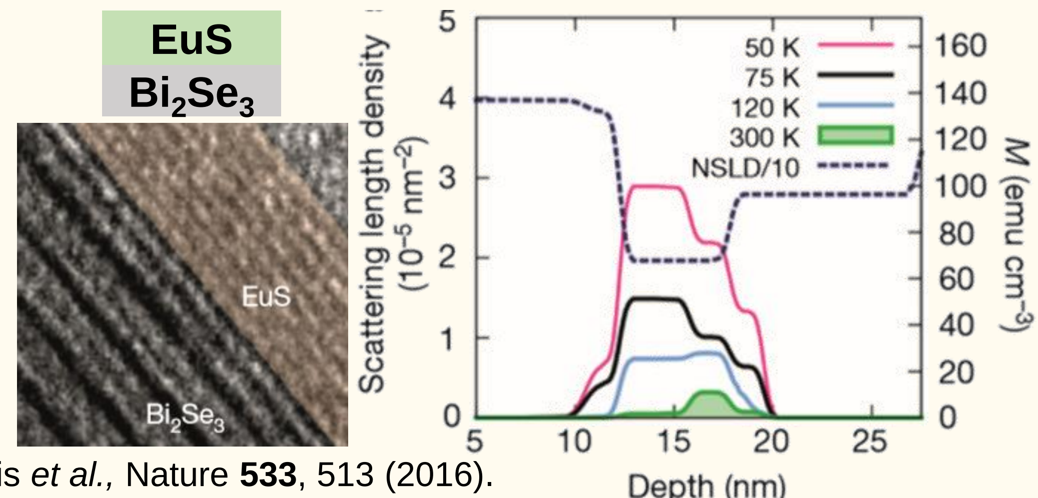

F. Katmis *et al.*, Nature **533**, 513 (2016).

Breaking TRS by MPE

Breaking Time Reversal Symmetry (TRS) in TIs

➡ Quantum anomalous Hall effect (QAHE)

Ways to break TRS in TIs:
Introducing magnetic moments

- **Transition metal doping**
- **Magnetic proximity effect (MPE)**

Magnetic proximity effect

Advantages of MPE:

- **Higher T_C than that of magnetic doping**
- **No crystal defects**
- **Uniform magnetization**

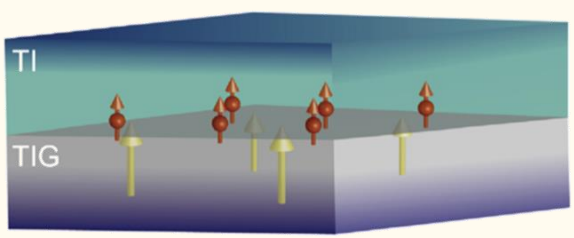

C. Tang *et al.*, Sci. Adv. **3** (6), e1700307 (2017).

Tensile-strained $Tm_3Fe_5O_{12}$ (thulium iron garnet, TmIG)

- **Magnetic insulator**
- **High T_C (above 500 K)**
- **Perpendicular magnetic anisotropy (PMA)**

C. N. Wu *et al.*, AIP Adv. **8** (5), 055904 (2018).
C. N. Wu *et al.*, Sci. Rep. **8** (1), 11087 (2018).

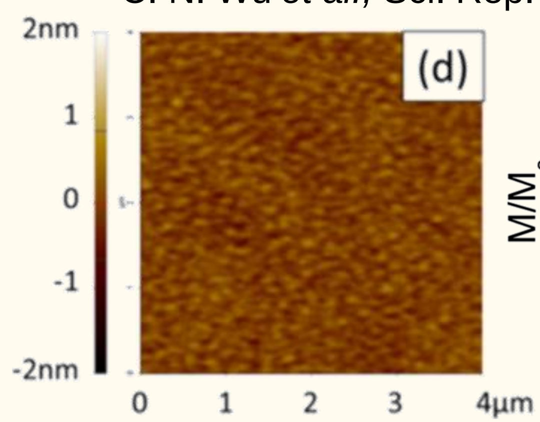

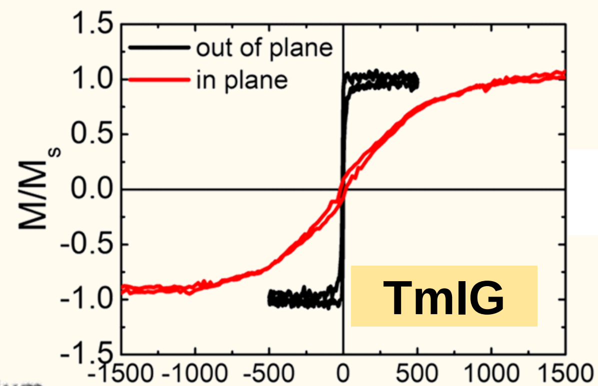

Breaking TRS by MPE

Breaking Time Reversal Symmetry (TRS) in TIs

➡ **Quantum anomalous Hall effect (QAHE)**

Ways to break TRS in TIs:
Introducing magnetic moments

➡ **Transition metal doping**

➡ **Magnetic proximity effect (MPE)**

However,

- **Complicated surface atomic arrangement**
- **Huge lattice mismatch with Bi_2Se_3**

Tensile-strained $Tm_3Fe_5O_{12}$ (thulium iron garnet, TmIG)

- **Magnetic insulator**
- **High T_C (above 500 K)**
- **Perpendicular magnetic anisotropy (PMA)**

C. N. Wu *et al.*, AIP Adv. **8** (5), 055904 (2018).
C. N. Wu *et al.*, Sci. Rep. **8** (1), 11087 (2018).

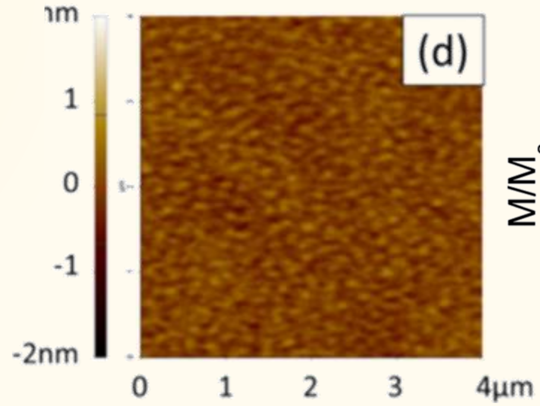

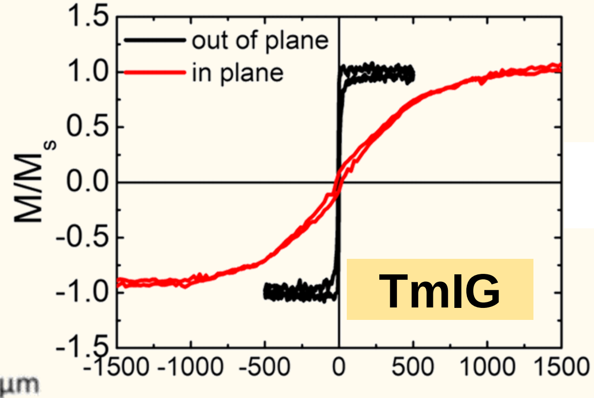

Breaking TRS by MPE

Conventional two-step growth

1st step: **Low temp.**

Ordered and smooth initial layer

2nd step: **High temp.**

Atoms with **more kinetic energy**

➡ Better film quality

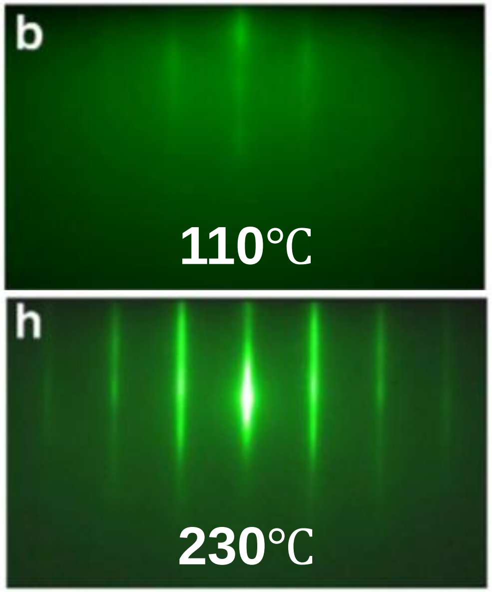

N. Bansal *et al.*, Thin Solid Films **520** (1), 224 (2011).

Applied on rare earth iron garnets (ReIGs):

➡ Atoms tend to **bond to the surface dangling bonds first**

Breaking TRS by MPE

Conventional two-step growth leads to:

Interlayer with poor crystallinity

H. Wang *et al.*, Phys. Rev. Lett. **117** (7), 076601 (2016).

Large variation of T_C of MPE properties

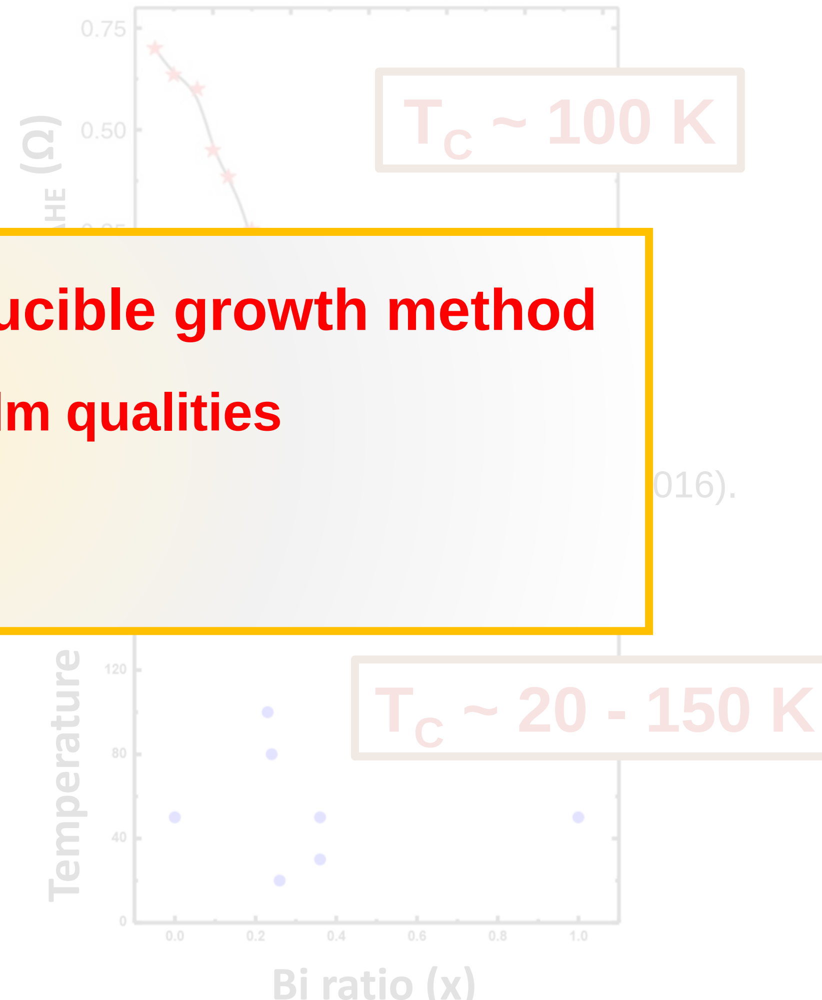

Z. Jiang *et al.*, Nano Lett. **15** (9), 5835 (2015).

Urgent demand for a reproducible growth method

- **Narrowing the variation of film qualities**
- **High-quality interface**
- **Strong exchange coupling**

Manipulating E_F toward Dirac point

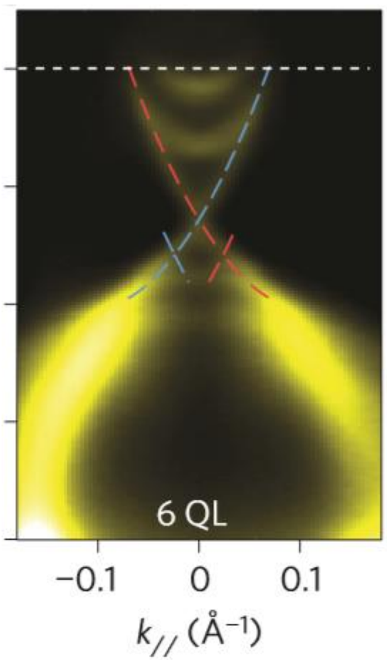

Y. Zhang et al., Nat. Phys. **6**, 584-588 (2010).

Bi_2Se_3

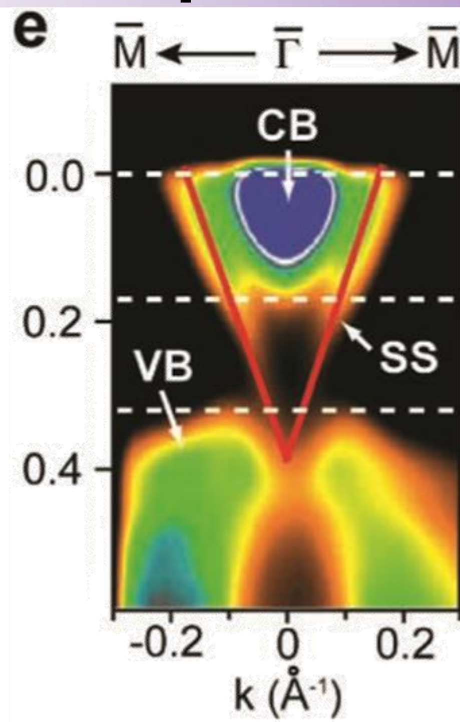

Y.-Y. Li *et al.*, Adv. Mater. **22**, 4002–4007 (2010).

Bi_2Te_3

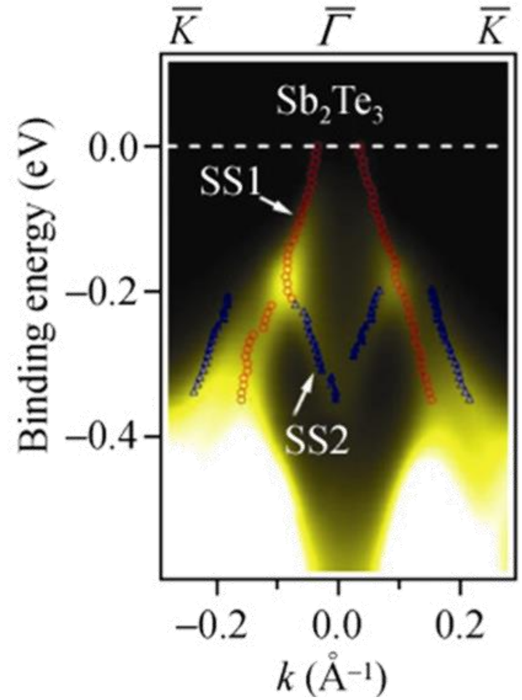

G. Wang *et al.*, Nano Res. **3**(12), 874–880 (2010).

Sb_2Te_3

Bulk c **and**

Su **es**

- **Bulk states dominate the transport properties.**
- **TSS features are diluted by the bulk contribution.**
- **It is hard to distinguish the contributions between the TSS and the bulk.**

Manipulating E_F toward Dirac point

Ways to eliminate/reduce the bulk contribution in TIs

→ **Electric gating effect**

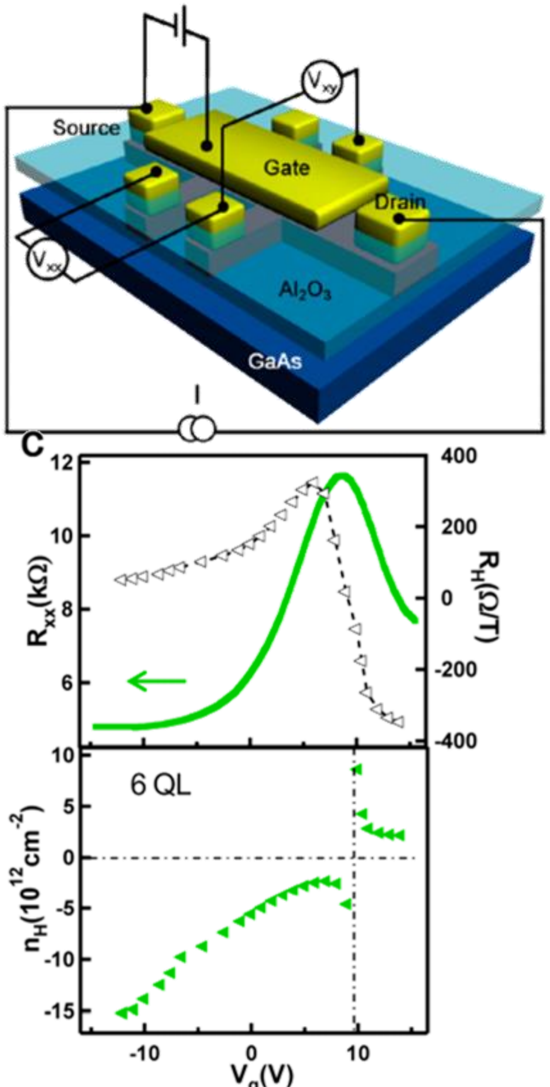

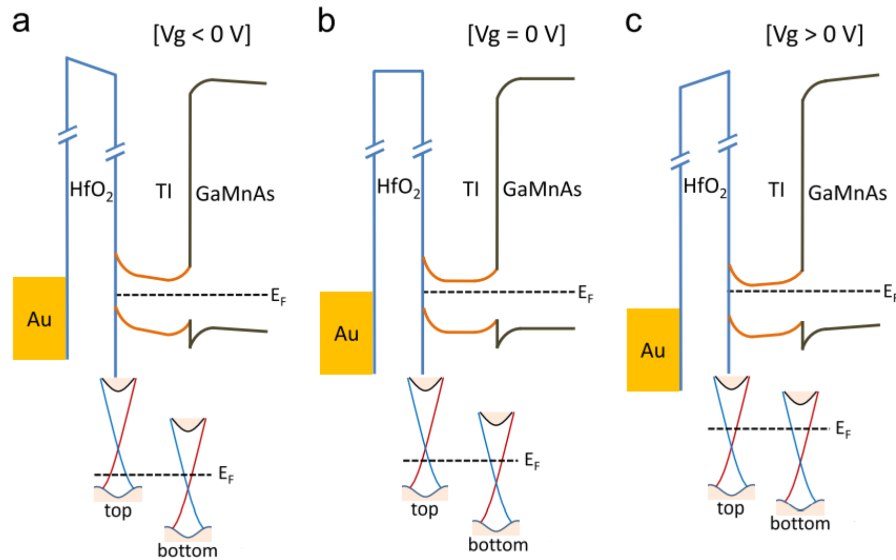

J. S. Lee *et al.*, npj Quantum Mater. **3**, 51 (2018).

M. Lang *et al.*, Nano Lett. **13**, 48−53 (2013).

Electric gating effect

- **Tuning E_F by the field effect**
- **Affecting only one side of the TI**
- **No modification on the band structure**

Manipulating E_F toward Dirac point

Ways to eliminate/reduce the bulk contribution in TIs

- **Electric gating effect**
- **Chemical doping / alloy**

$(Bi,Sb)_2Te_3$ (BST)

- **Tuning the position of the E_F**
- **Introducing different amounts of defects**
- **Modifying the band structure of TI**

Bi_2Te_3	Sb_2Te_3
Te_{Bi} anti-site	Sb_{Te} anti-site
↓	↓
n-type doping	p-type doping

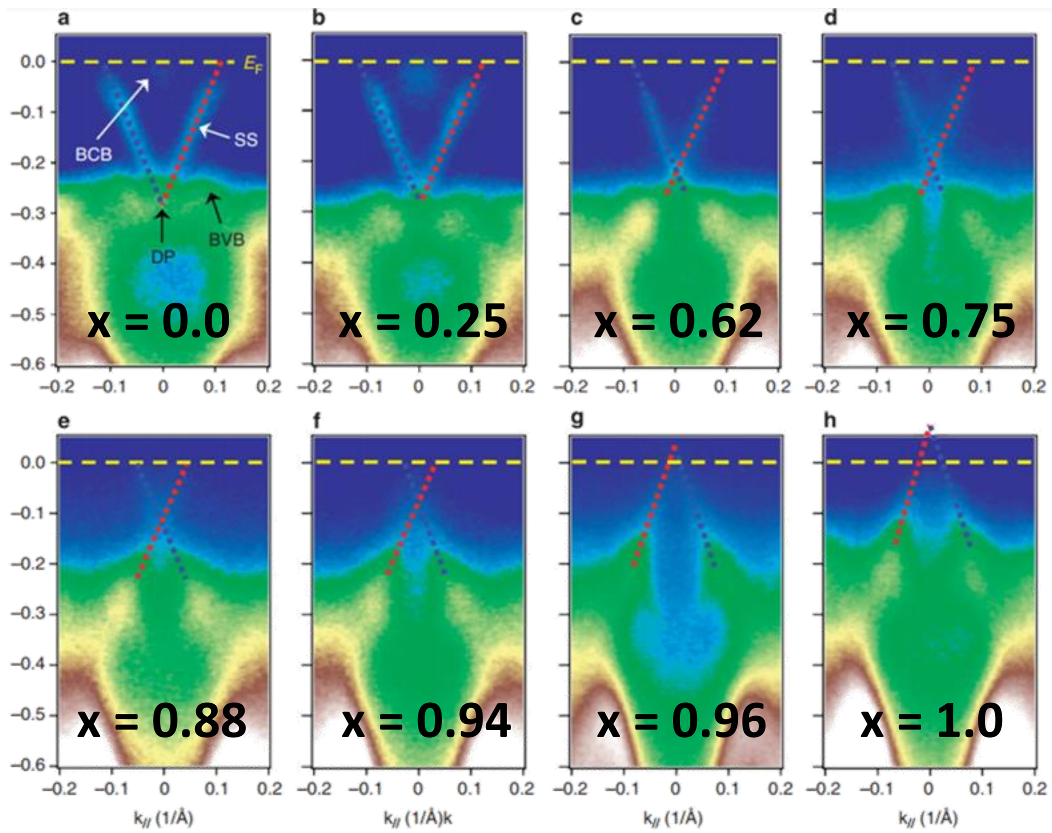

J. Zhang, *et al.*, Nat. Commun. **2**, 574 (2011).
J. M. Zhang *et al.* Phys. Rev. B **88**, 235131 (2013)

Manipulating the E_F into the bulk band gap ➡ bulk insulating TI

Motivation

Molecular Beam Epitaxy (MBE)

Base pressure:
4×10^{-10} torr
(2×10^{-10} torr)

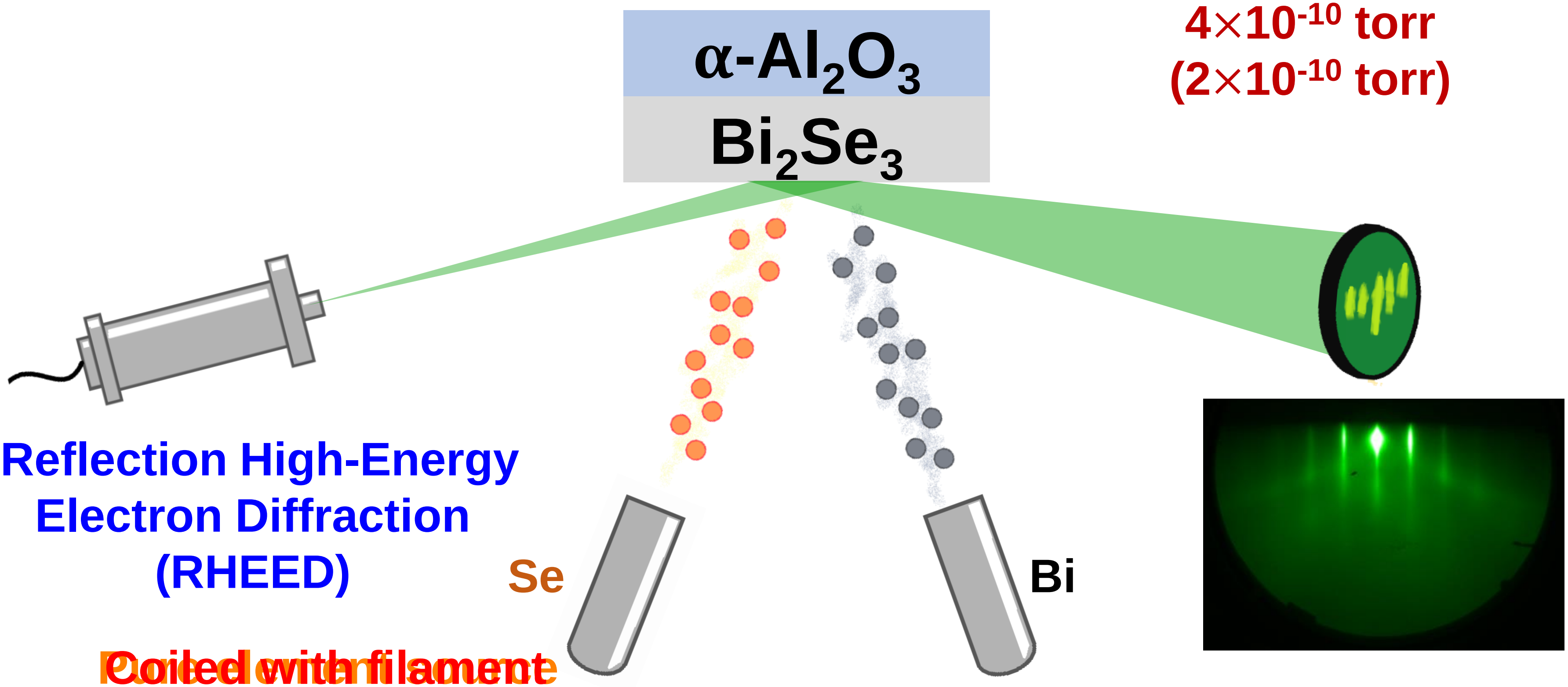

Reflection High-Energy Electron Diffraction (RHEED)

Coiled with filament

2D diffraction

Streaks: smooth surface & Great crystallinity

Rings or Spots: polycrystalline or rough surface

Motivation

Bi_2Se_3

α-Al_2O_3

$(Bi,Sb)_2Te_3$

α-Al_2O_3

- **Toward bulk-insulting feature**
- **Exhibition of pure surface state**

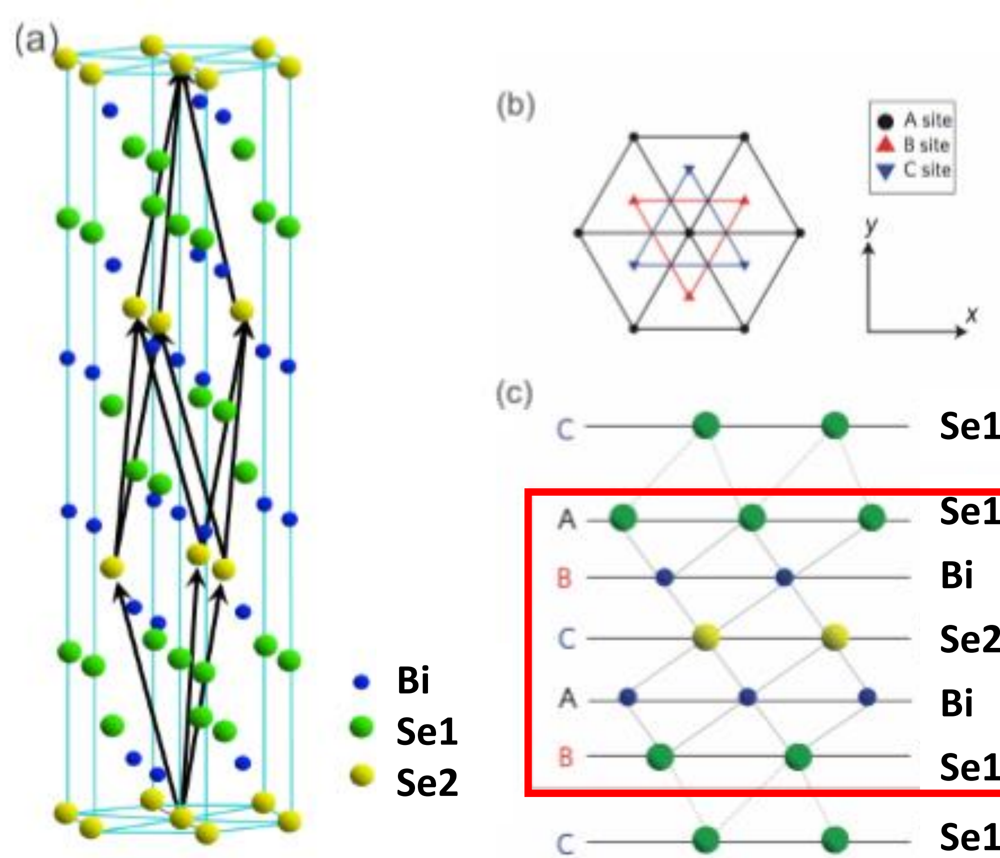

H. Zhang *et al.*, Nat. Phys. **5** (6), 438 (2009).

Quintuple layer (QL) (~ 1 nm)

TmIG

- **Breaking time reversal symmetry**
- **Pushing the T_C up to room temperature**

I: Bi_2Se_3/TmIG & Bi_2Se_3/YIG

- **Bi_2Se_3 / Rare earth iron garnet (ReIG)**
  - Advantage of ReIGs
  - Growth method: Se-buffered low-temperature (SBLT) growth
  - Improvement in crystallinities (vs. conventional two-step growth)
  - Enhancement of interfacial exchange coupling

ReIG substrate preparation

- Thulium iron garnet ($Tm_3Fe_5O_{12}$, TmIG)
  - Perpendicular magnetic anisotropy (PMA) (induced by tensile strain)
- Yttrium iron garnet ($Y_3Fe_5O_{12}$, YIG)
  - In-plane magnetic anisotropy (IMA) and low damping constant

Sputter → Without chemical cleaning → **MBE**

a)

Outgassing

Bi_2Se_3/YIG at 500℃

H. Wang *et al.*, Phys. Rev. Lett. **117**, 076601 (2016).

$(Bi,Sb)_2Te_3$/YIG at 600℃, 1hr

Z. Jiang *et al.*, AIP Adv. **6**, 055809 (2016).

$(Bi,Sb)_2Te_3$/TmIG at 600℃, 1hr

C. Tang et al., Sci. Adv. **3** (6), e1700307 (2017).

Outgassing

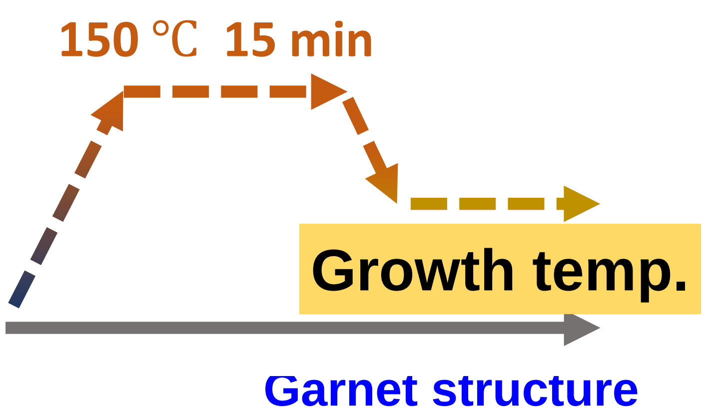

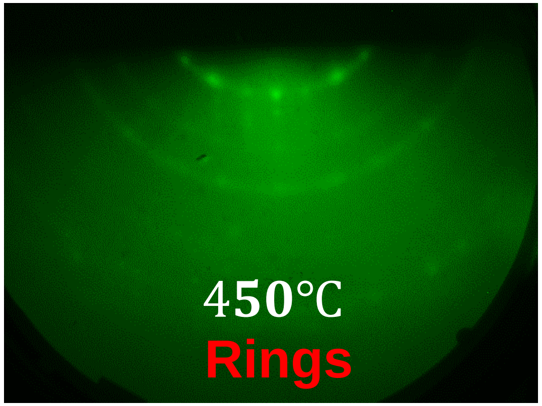

RHEED patterns:
350℃↑ ring (polycrystalline)

Residual gas analysis:
300℃↑ C_xO_x compounds

Demand for a reproducible growth method

However,

- Complicated surface atomic arrangement
- Huge lattice mismatch with Bi_2Se_3

Interlayer with poor crystallinity

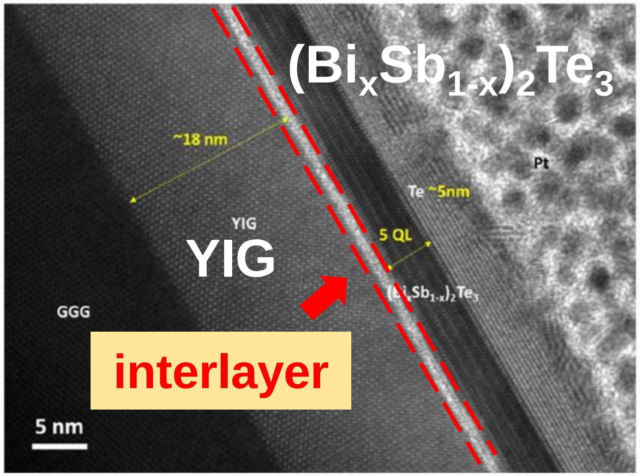

Z. Jiang *et al.*, AIP Adv. **6** (5), 055809 (2016).

Conventional two-step growth

1st step: Low temp.

Ordered and smooth initial layer

2nd step: High temp.

Atoms with more kinetic energy

➡ Better film quality

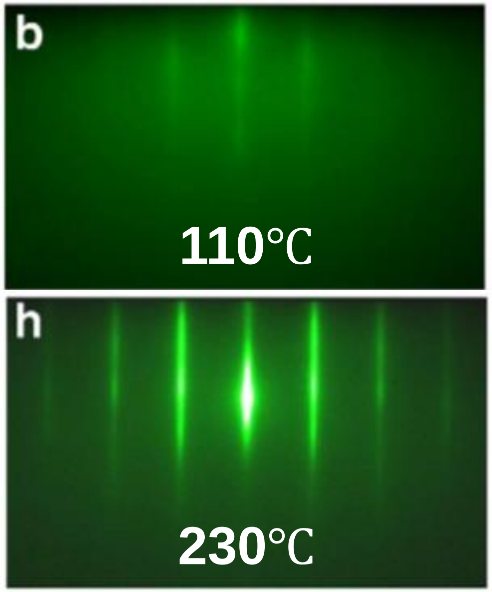

N. Bansal *et al.*, Thin Solid Films **520** (1), 224 (2011).

Urgent demand for a reproducible growth method

- Narrowing the variation of film qualities
- High-quality interface
- Strong exchange coupling

The SBLT growth

The Se-buffered low-temperature (SBLT) growth:

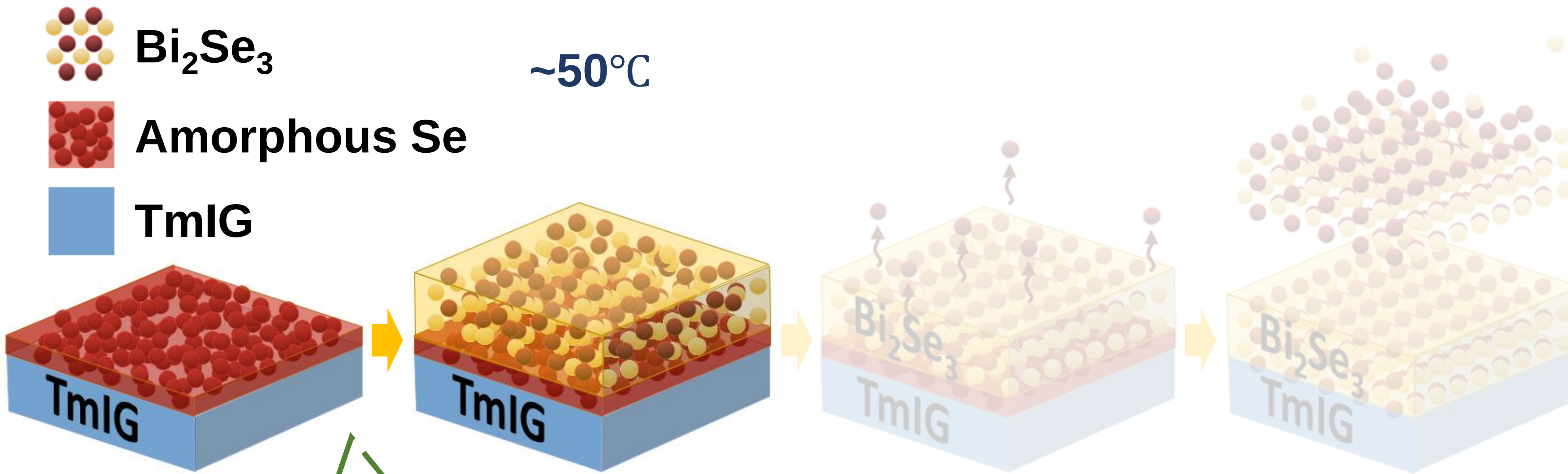

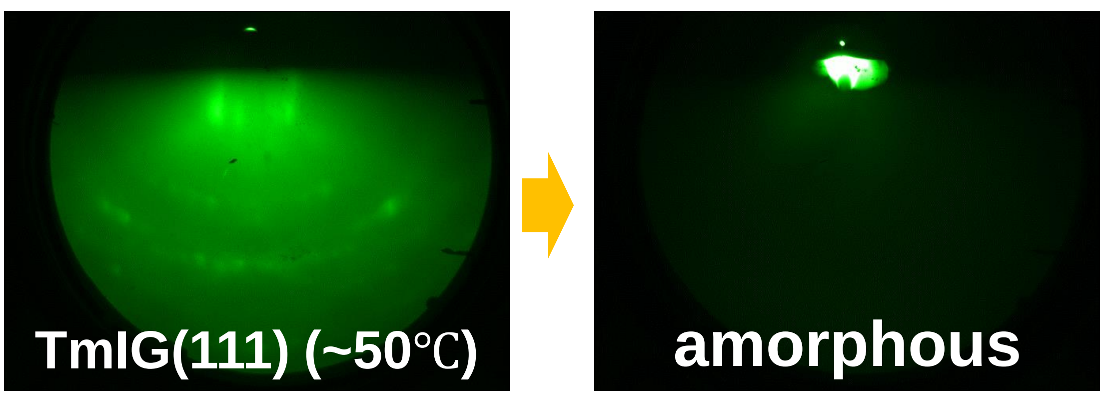

The substrate was covered by a layer of **amorphous Se** and **~1 nm Bi_xSe_{1-x}**.

The SBLT growth

The Se-buffered low-temperature (SBLT) growth:

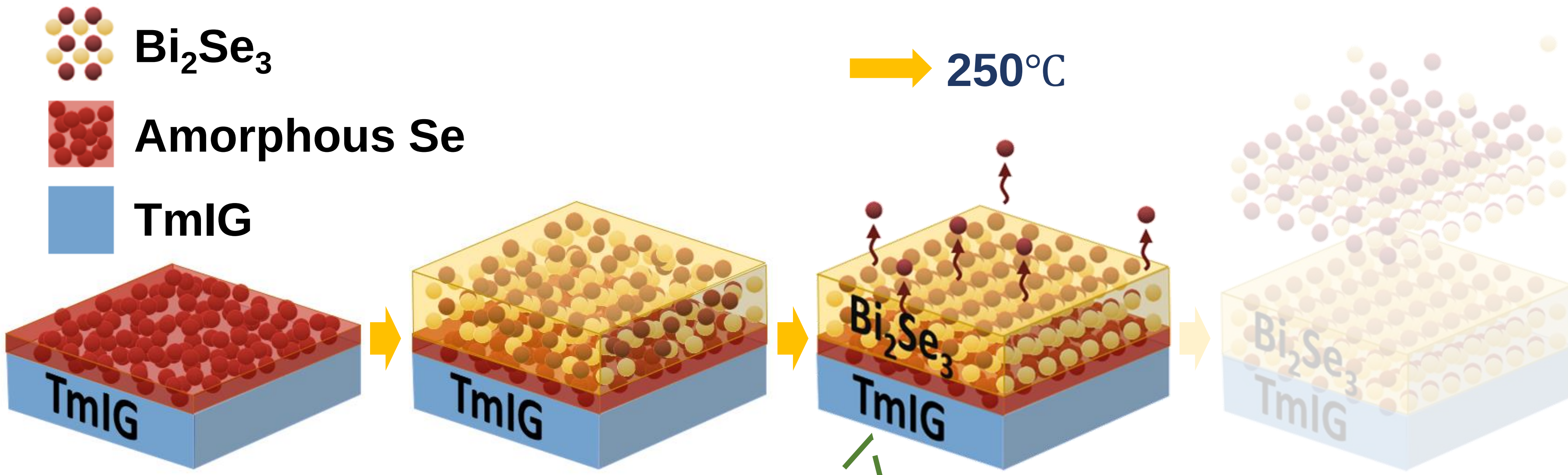

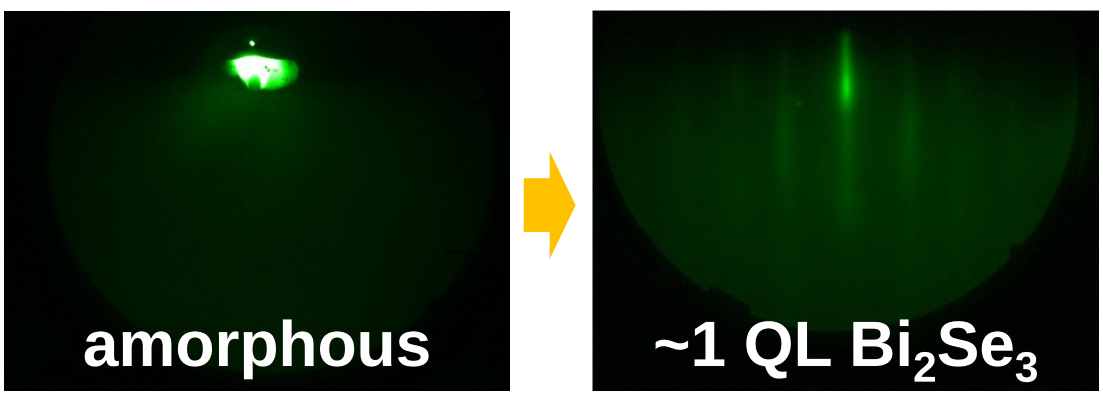

The **high-quality Bi_2Se_3 at the 1st QL** serves as **a great template** for the further Bi_2Se_3 growth.

The SBLT growth

The Se-buffered low-temperature (SBLT) growth:

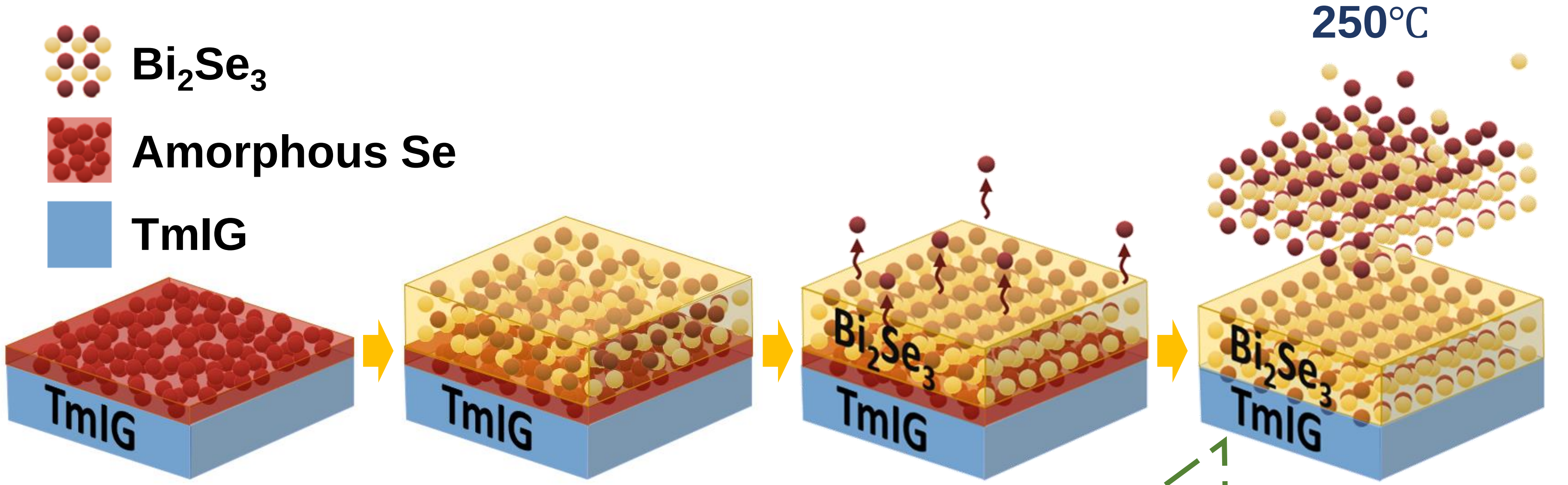

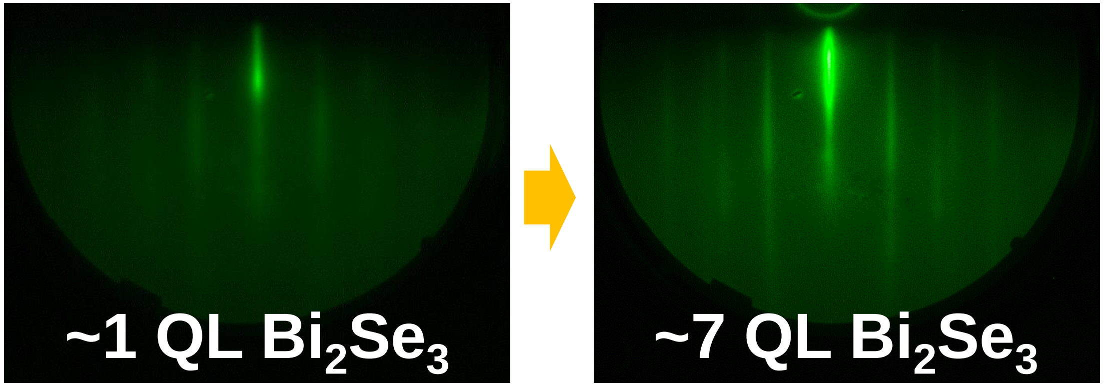

Sharper and brighter RHEED patterns were obtained in thicker Bi_2Se_3 films.

Comparison of RHEED patterns

Spotty ring feature
➡ poly crystalline

Grain growth,
forming 2D surface

Reaching a good-quality surface

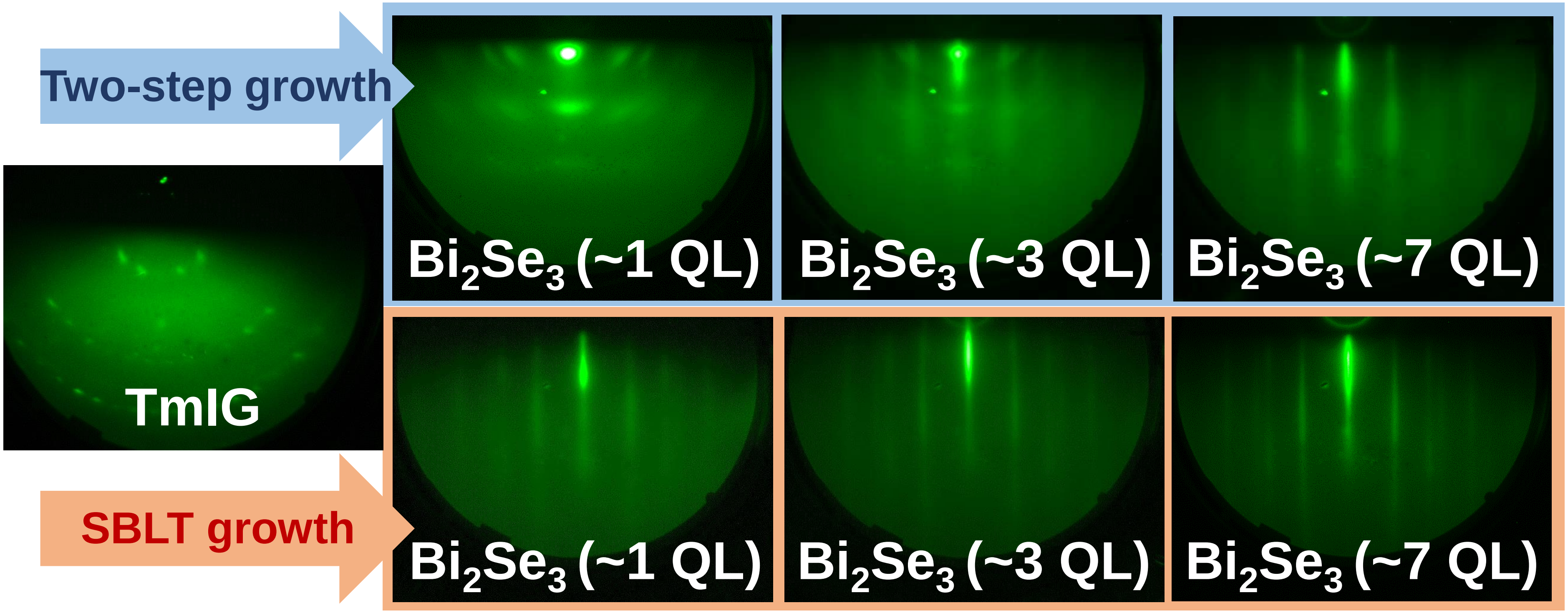

Line feature
➡ better crystallinity
and smooth surface

More distinct RHEED patterns
➡ achieving excellent crystallinity of thin films

Comparison of RHEED patterns

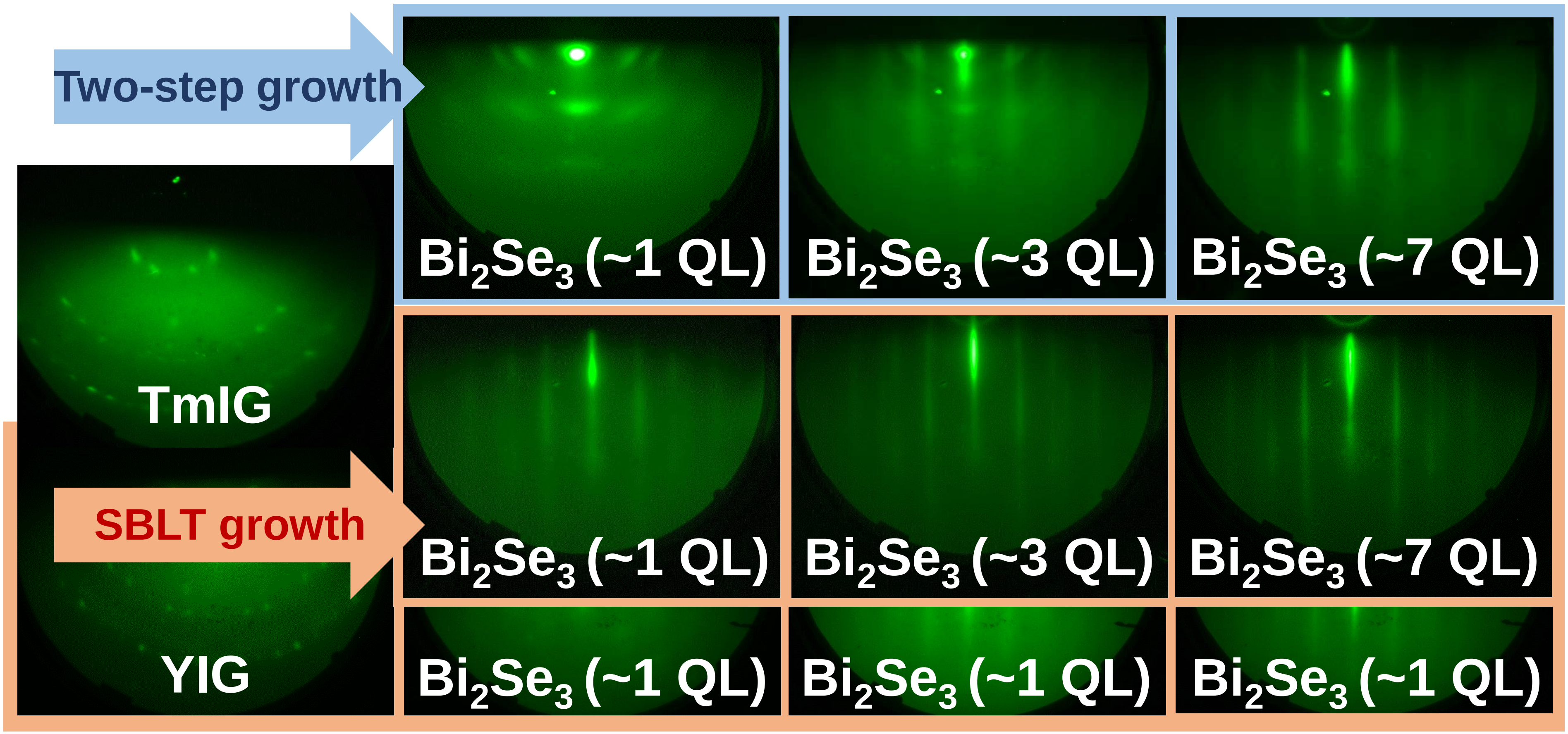

It works on Bi_2Se_3/YIG !

Structural analyses

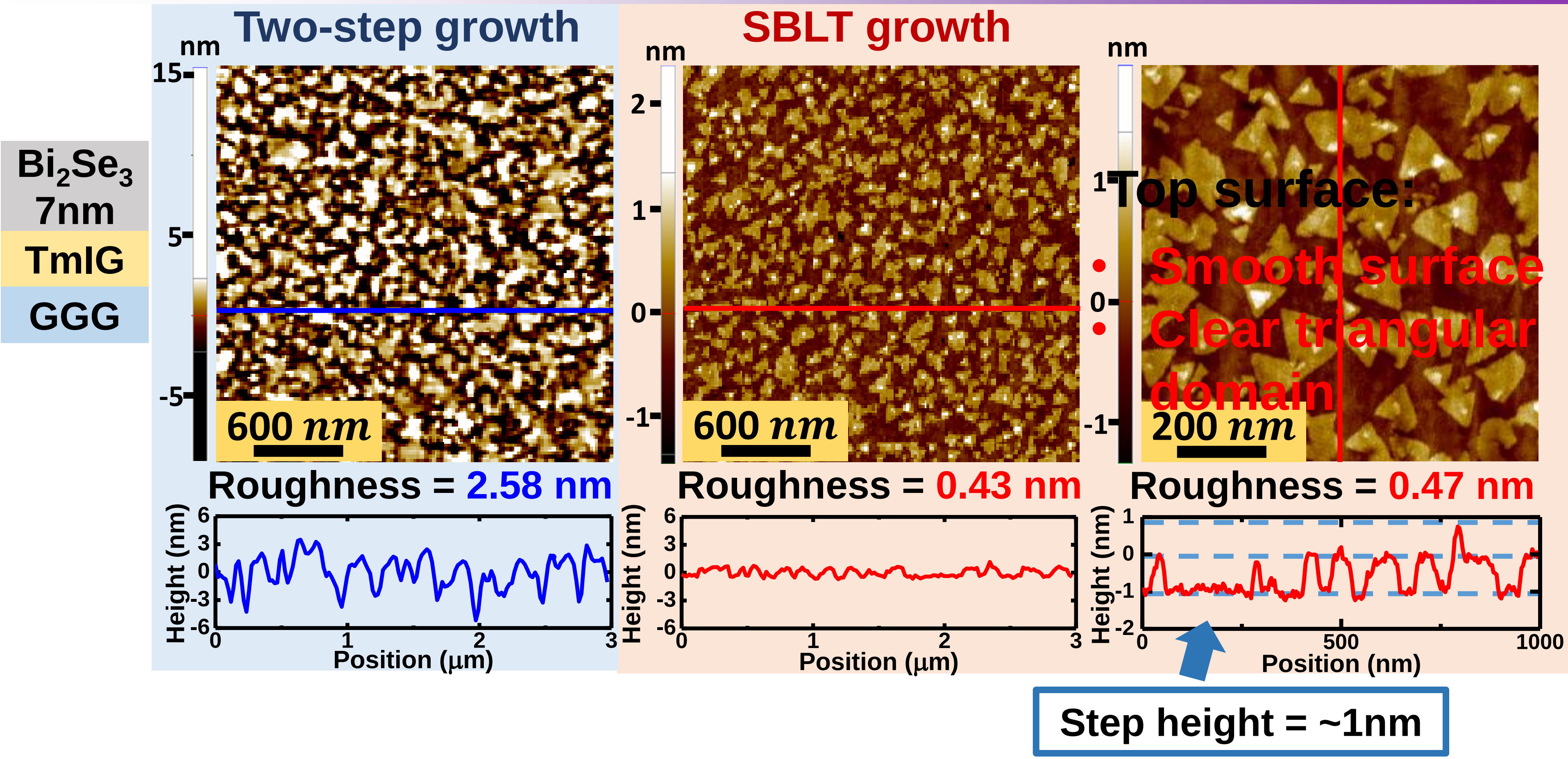

Structural analyses

Two-step growth	SBLT growth

Bi_2Se_3 7nm
TmIG
GGG

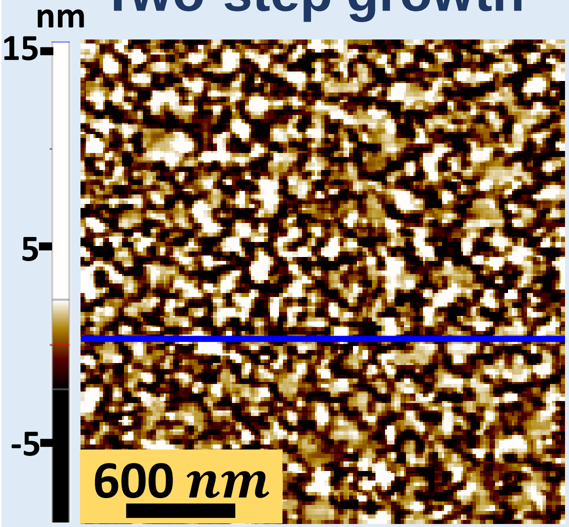

Roughness = 2.58 nm

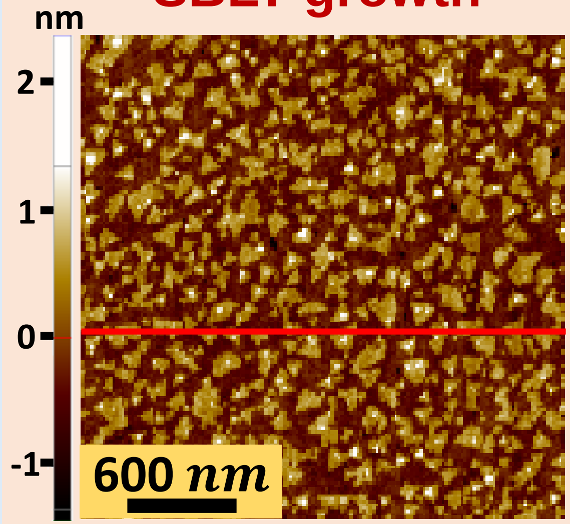

Roughness = 0.43 nm

Top surface:

- Smooth surface
- Clear triangular domain

Bi_2Se_3 7nm
YIG
GGG

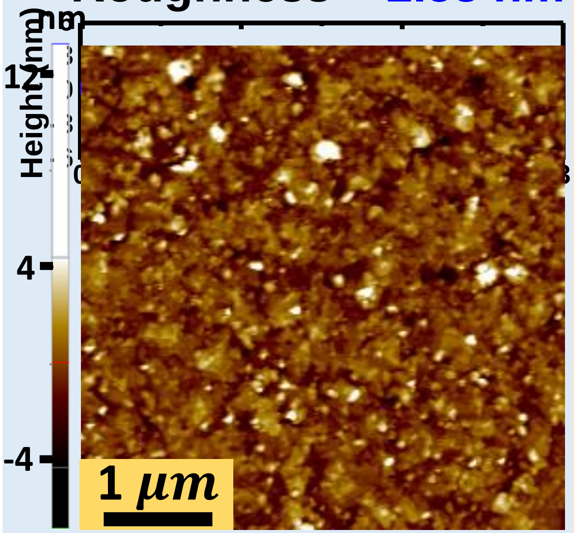

Roughness = 1.29 nm

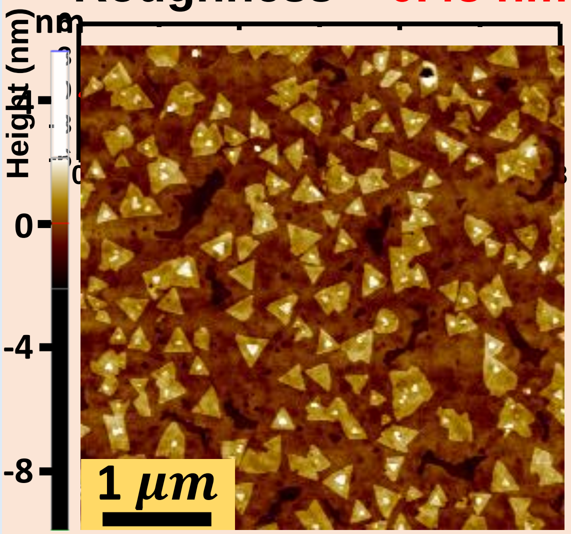

Roughness = 0.58 nm

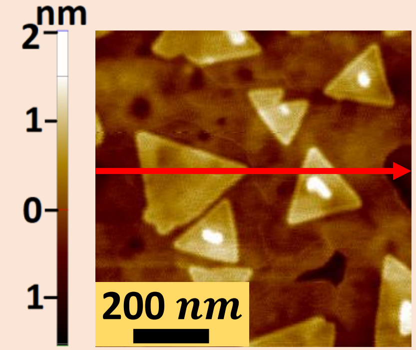

Roughness = 0.47 nm

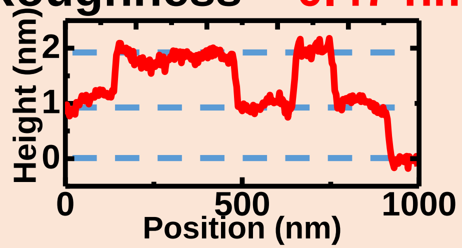

Structural analyses

Two-step growth

Bi_2Se_3 7nm
TmIG
GGG

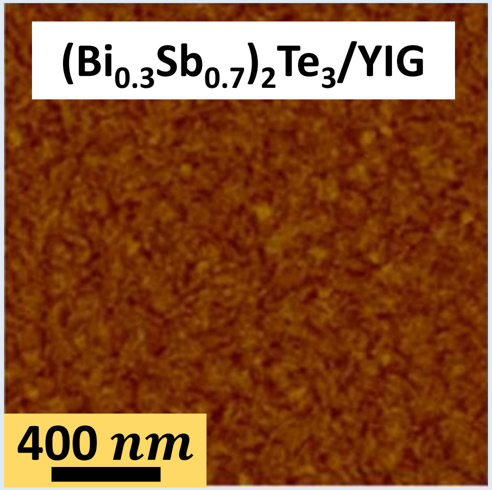

Roughness = 0.77 nm

C. Tang *et al.*, Sci. Adv. **4**, eaas8660 (2018).

Bi_2Se_3 7nm
YIG
GGG

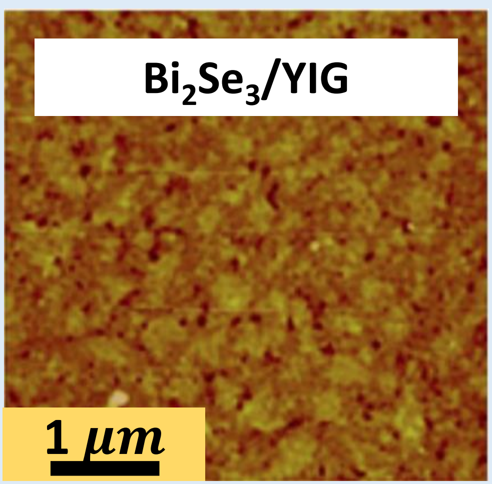

Roughness = 0.71 nm

H. Wang *et al.*, Phys. Rev. Lett. **117** (7), 076601 (2016).

SBLT growth

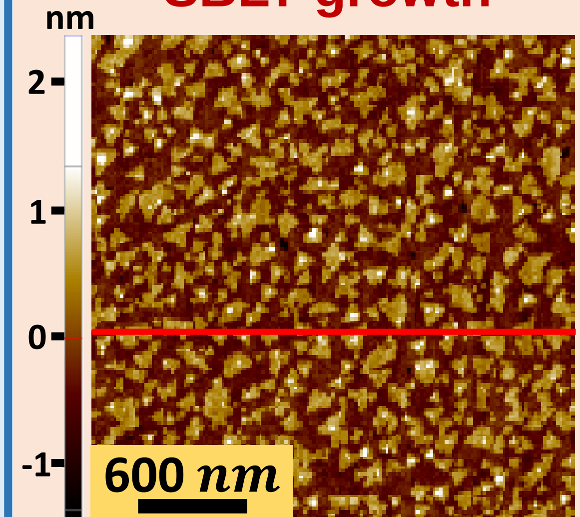

Roughness = 0.43 nm

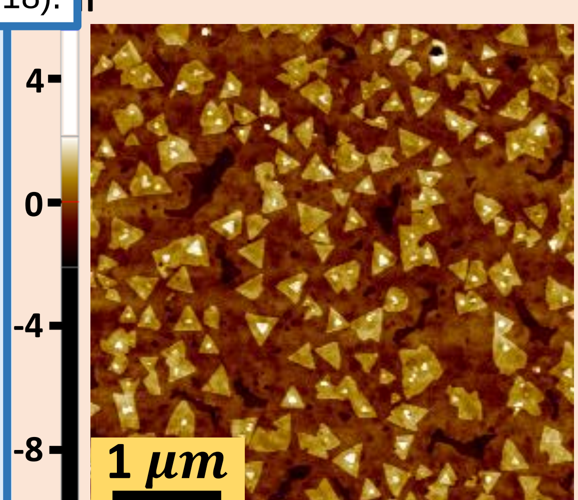

Roughness = 0.58 nm

Top surface:

- Smooth surface
- Clear triangular domain

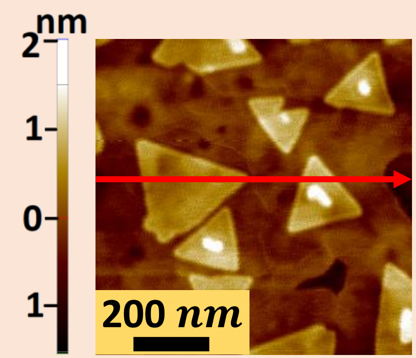

Roughness = 0.47 nm

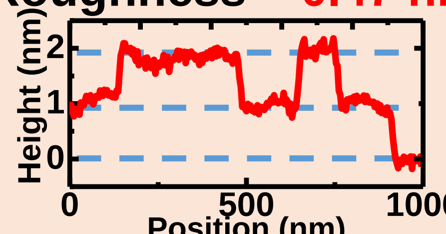

Structural analyses

HRTEM images

Cs-corrected STEM images

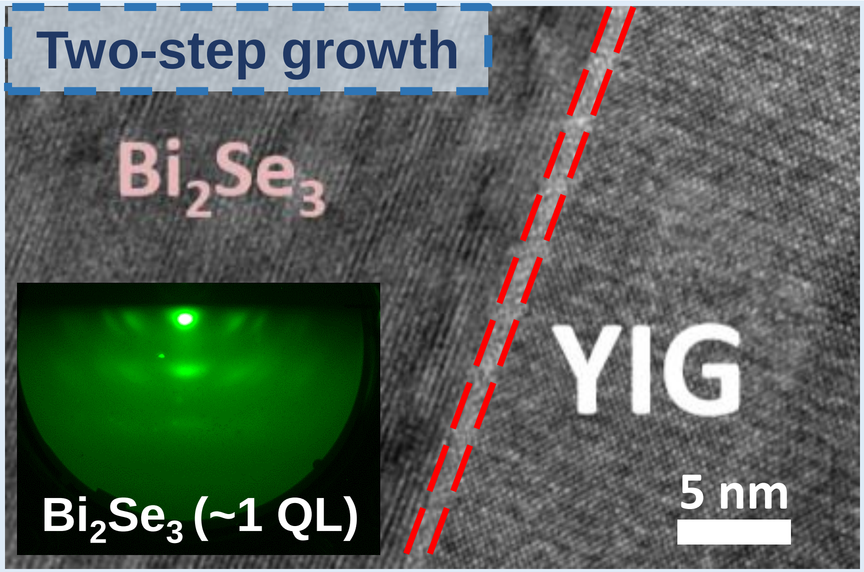

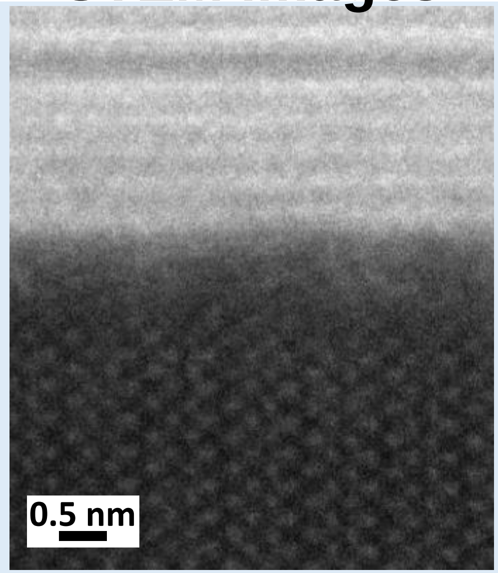

Interface:

- ~1nm amorphous interlayer

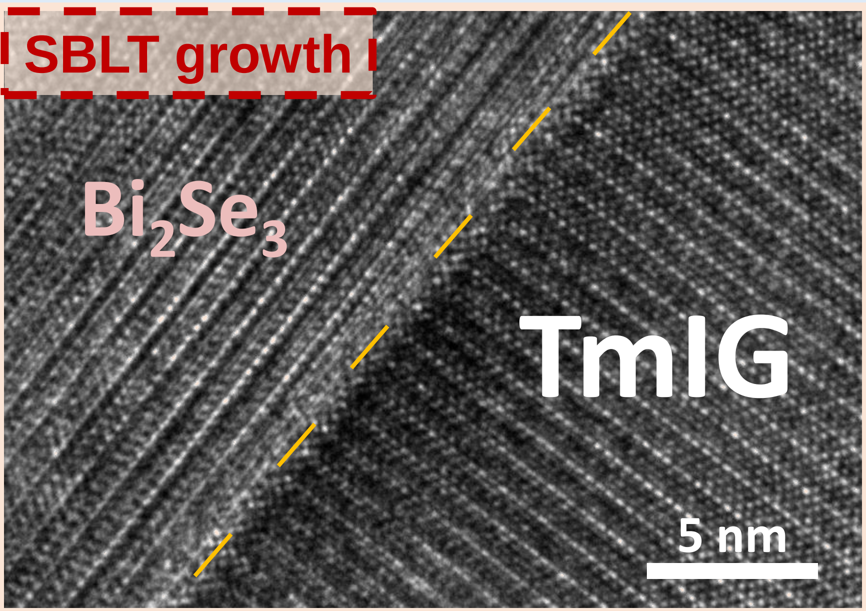

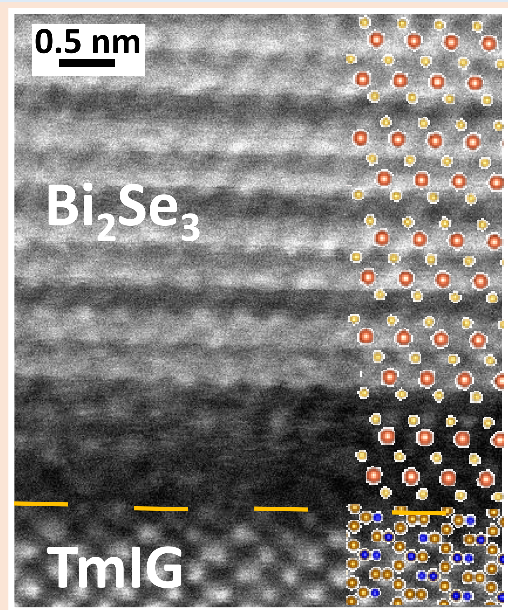

Films:

- Clear atomic structures

Interface:

- Se buffer layer evaporated
- Visible atoms in the 1st QL

Interfacial analyses

XPS spectra of 4 nm Bi_2Se_3 on TmIG

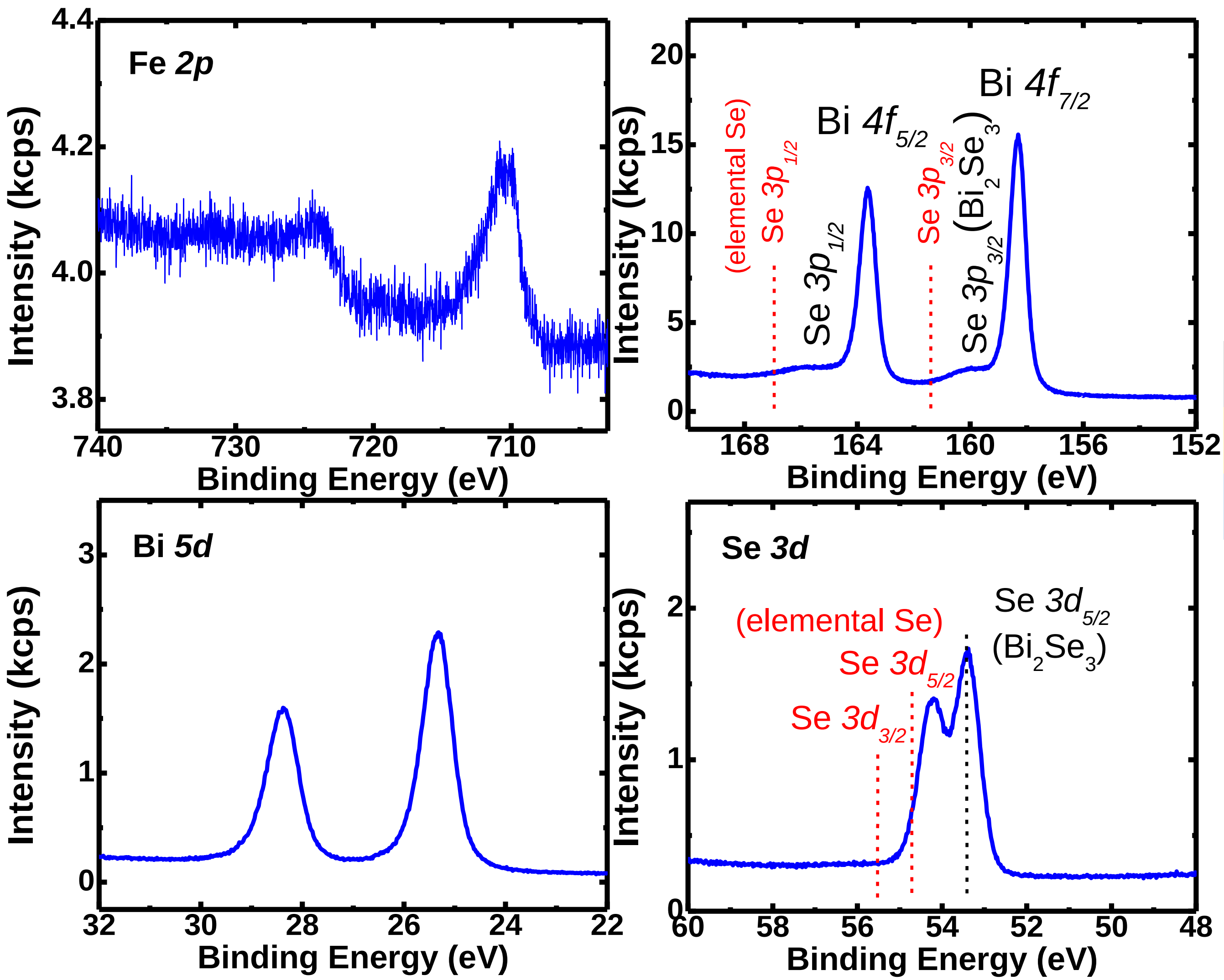

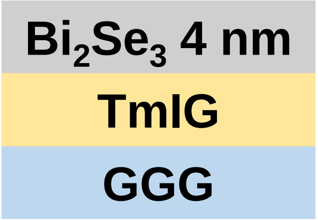

No elemental Se was detected at the interface!

Observation of AHE

Bi_2Se_3
TmIG
GGG

Anomalous Hall effect (AHE) loops

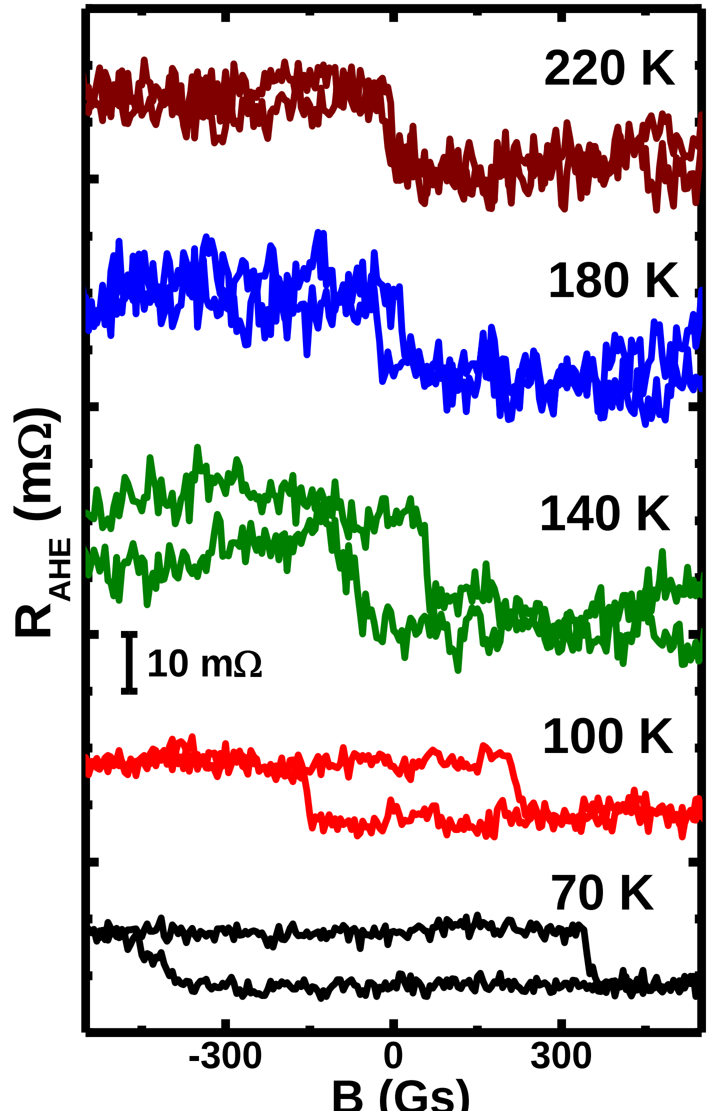

Magnetic proximity effect (MPE):

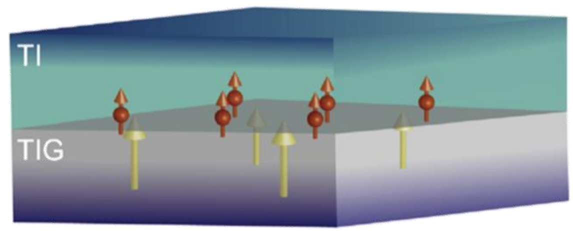

Magnetization of the bottom topological surface state (TSS)

C. Tang et al., Sci. Adv. **3** (6), e1700307 (2017).

Spin current effect has been precluded in our other work

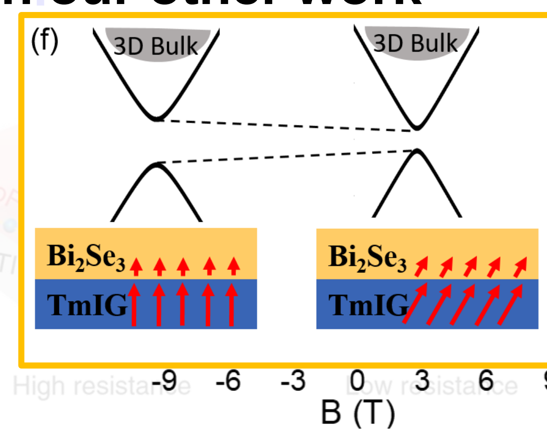

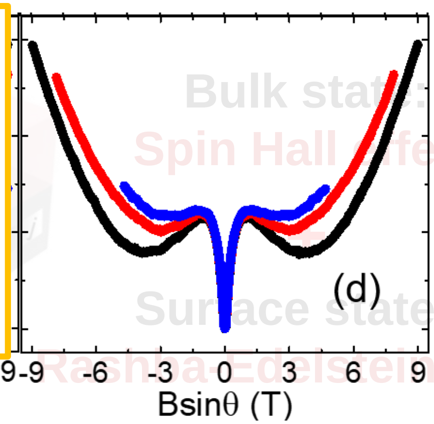

S. R. Yang et al., arXiv: 1811.00689 (2018).
(Accepted by Phys. Rev. B)

Enhanced exchange coupling at the interface!

Enhanced interfacial exchange coupling

Two-step growth

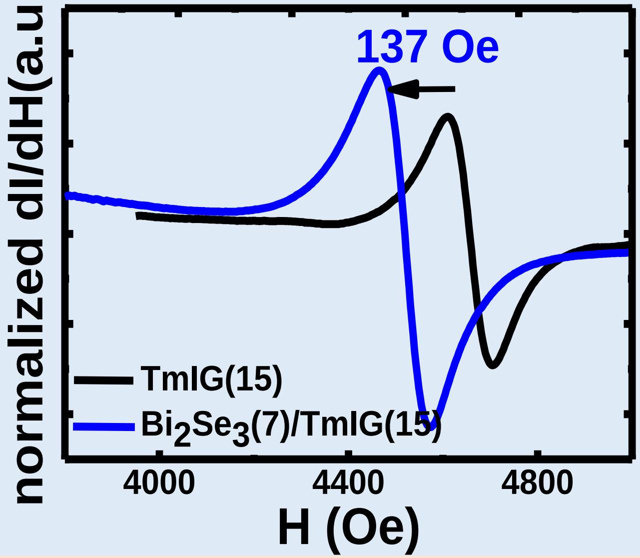

SBLT growth

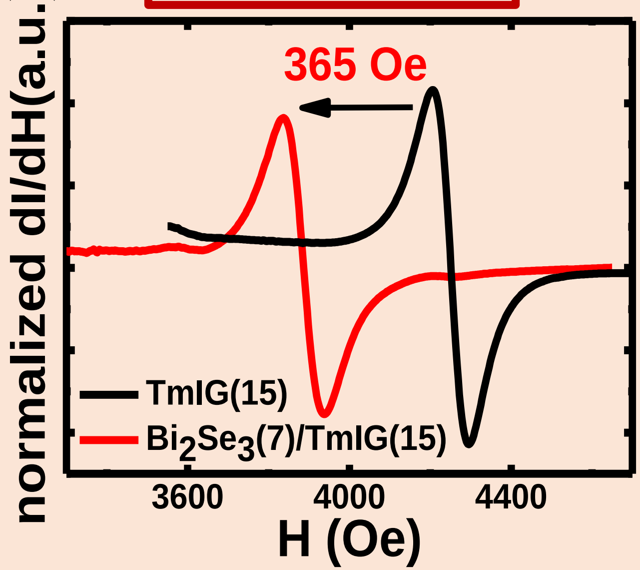

Our previous work

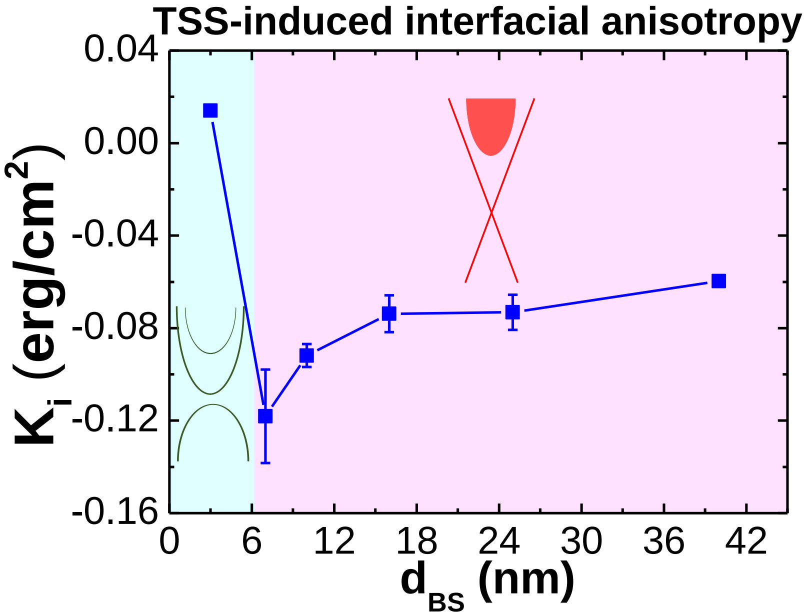

Y. T. Fanchiang et al., Nat. Commun. **9**, 223 (2018)

Ferromagnetic resonance (FMR)

Spin dynamics at the **interface**

Bi_2Se_3 grown on TmIG

Negative shift in H_{res} of TmIG

Enhancement of **IMA** at the interface

Stronger interfacial exchange coupling !

Summary I

Our SBLT growth attained:

- Bright and distinct RHEED at the 1st QL
- Smoother surface and sharp triangular domains
- High-quality interface
- Observation of AHE
- Larger shift in H_{res}

} Enhan … ge

C. C. Chen *et al.,* Appl. Phys. Lett. **114**, 031601 (2019).
(Featured, cover story)

II: $(Bi,Sb)_2Te_3/\alpha\text{-}Al_2O_3$ & $(Bi,Sb)_2Te_3$/TmIG

- **$(Bi,Sb)_2Te_3$ / $\alpha\text{-}Al_2O_3$ & $(Bi,Sb)_2Te_3$ / TmIG**
  - Characterization of structural properties
  - Evidences of **manipulating E_F** toward **bulk-insulating features**
  - Electronic transport & magnetoresistance analysis

Manipulating E_F toward Dirac point

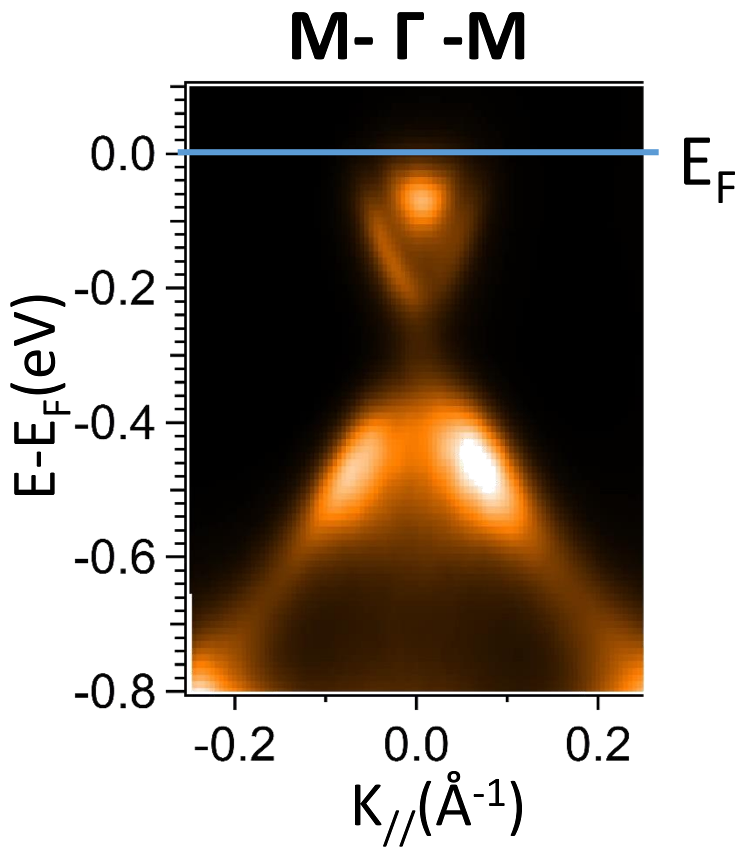

Bi_2Se_3 (our work)

Bulk conduction band
+
Surface states

- **Bulk states dominate the transport properties.**
- **It is hard to distinguish the contributions between the TSS and the bulk.**

Ways to eliminate/reduce the bulk contribution in TIs: $(Bi,Sb)_2Te_3$

- **Tuning the position of the E_F**
- **Introducing different amounts of defects**
- **Modifying the band structure of TI**

Bi_2Te_3	Sb_2Te_3
Te_{Bi} anti-site	Sb_{Te} anti-site
⬇	⬇
n-type doping	p-type doping

J. M. Zhang *et al.* Phys. Rev. B **88**, 235131 (2013)

Manipulating the E_F into the bulk band gap bulk insulating TI

Excellent crystallinities of BST films

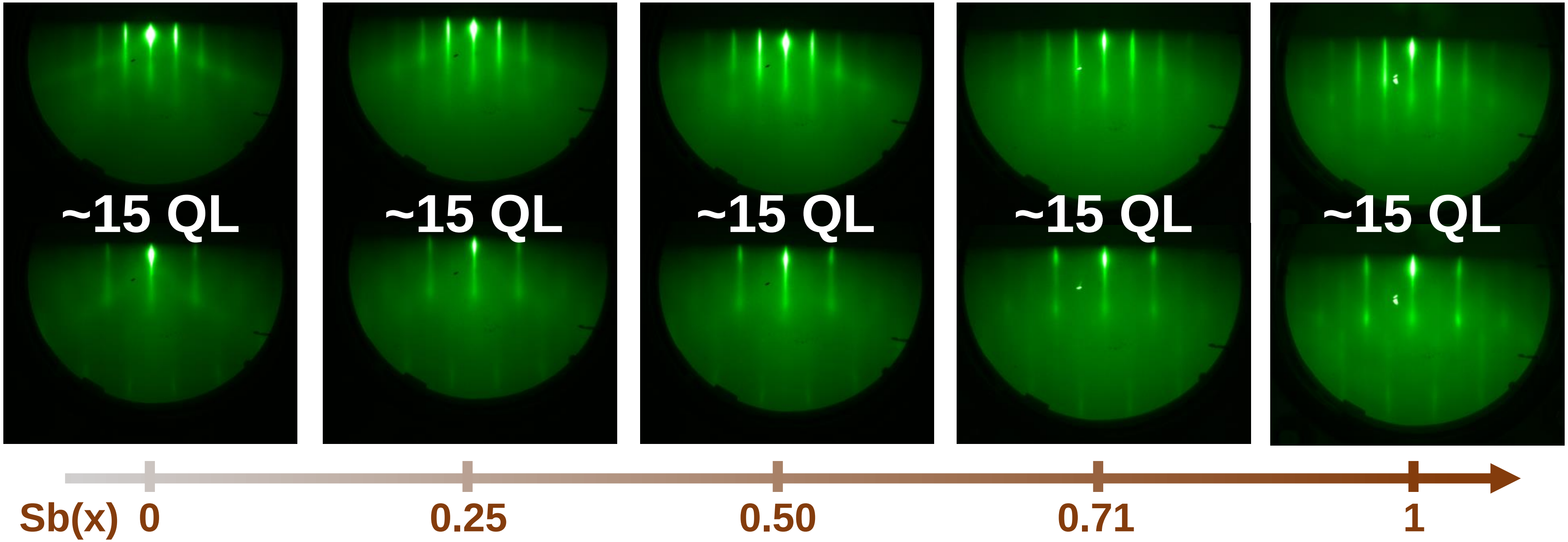

- **Streaky RHEED patterns** from the **very first quintuple layer** (QL) to ~15 QL grown by **MBE**

Excellent crystallinities of BST films

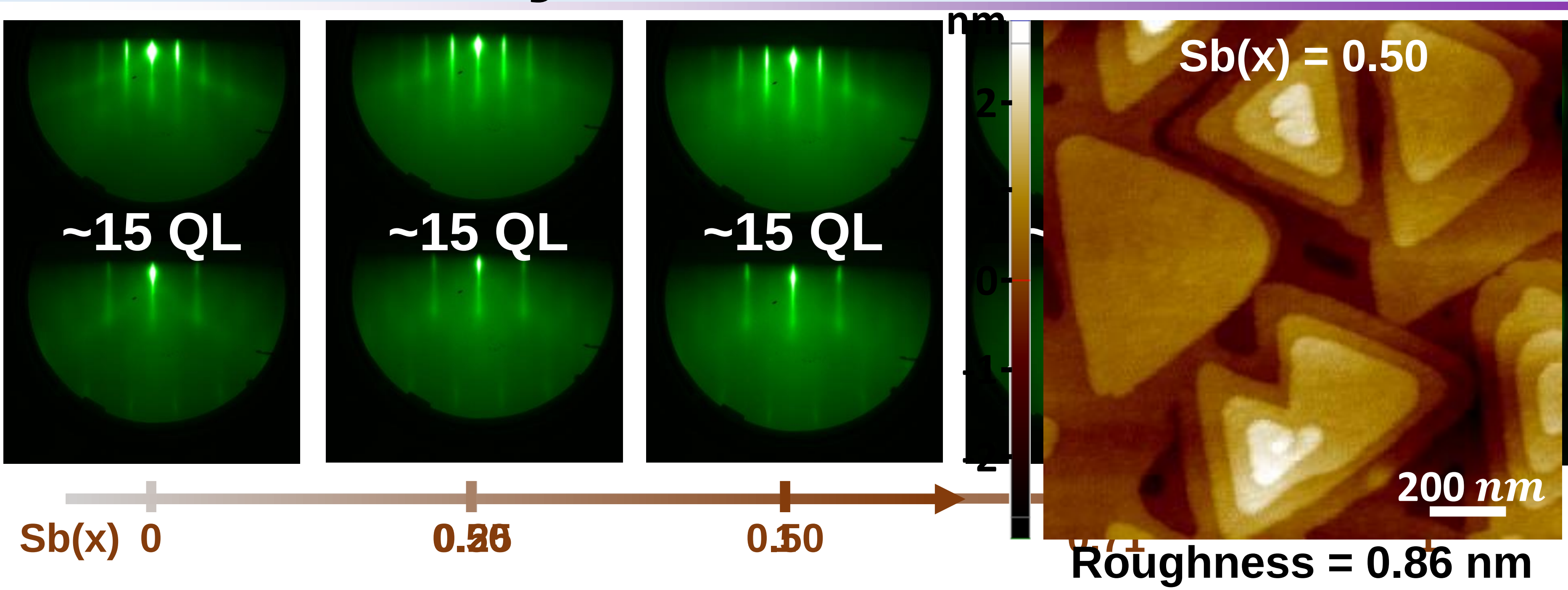

- **Streaky RHEED patterns** from the **very first QL** to ~15 QL grown by **MBE**
- **Large domains** with **sharp triangular shapes**
- **Clear RHEED oscillations** indicating **the layer-by-layer growth**

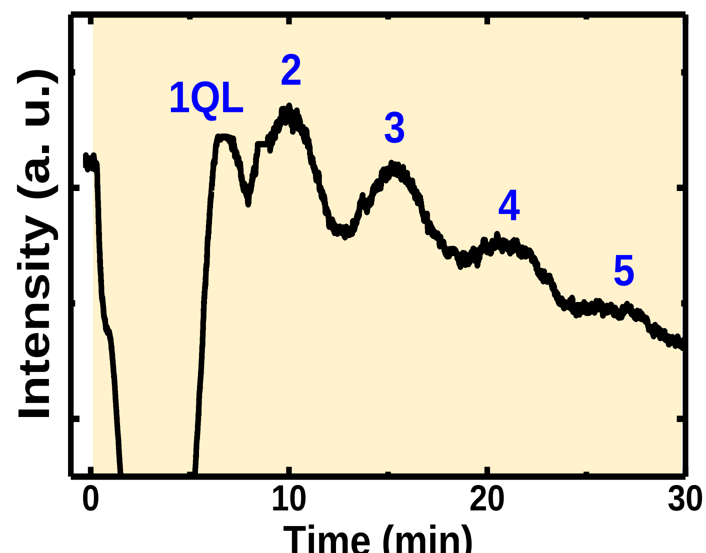

Composition characterization

XRD (*ex-situ*)

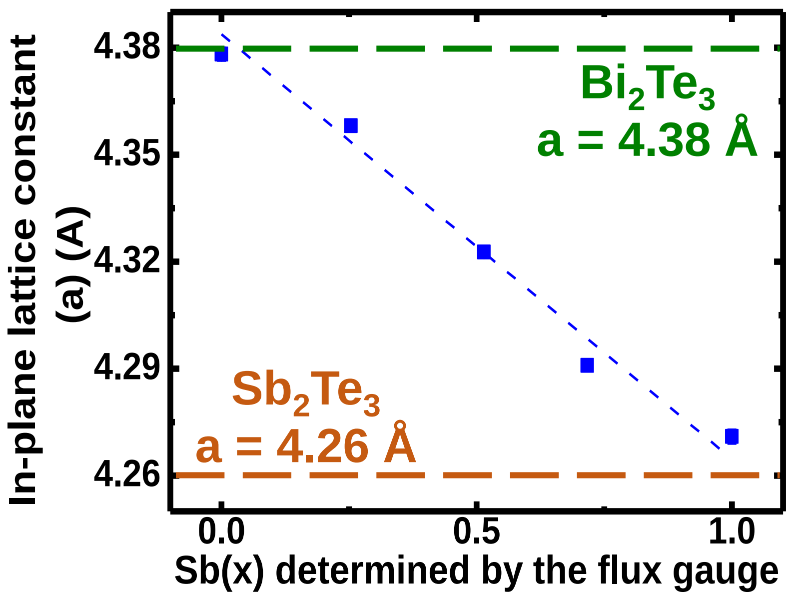

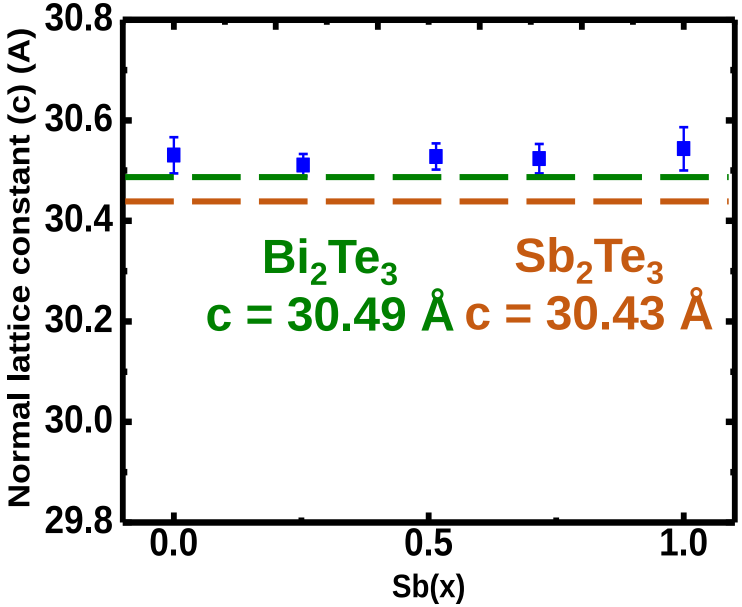

XPS (*in-situ*)

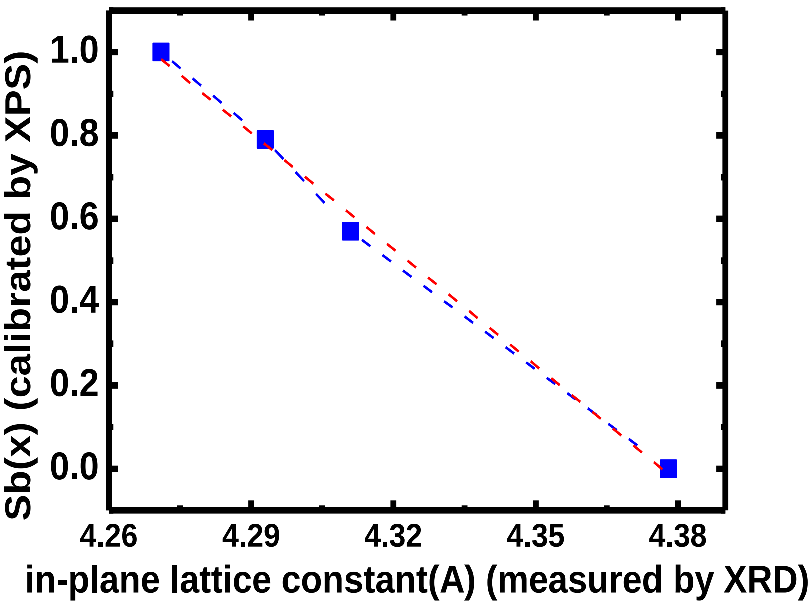

- Compositions of $(Bi,Sb)_2Te_3$ can be both ***in-situ*** and ***ex-situ*** calibrated by **X-ray photoelectron spectroscopy (XPS)** and **X-ray diffraction (XRD)**, respectively.

Te capping layer & R-T curves

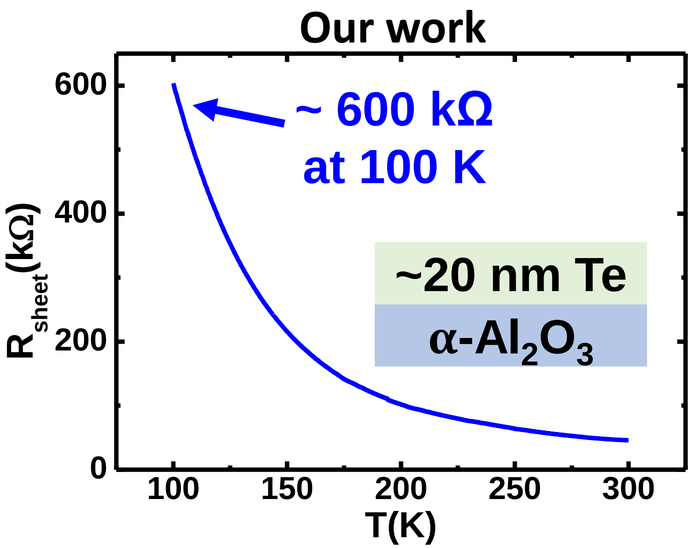

At 300 K

$n_{2D} = 3.37\times10^{12}$ cm^{-2}

R_{sheet} = 45483 Ω

Mobility = 39.8 cm^2/Vs

~20 nm Te

$(Bi,Sb)_2Te_3$

α-Al_2O_3

To prevent the oxidation of TIs

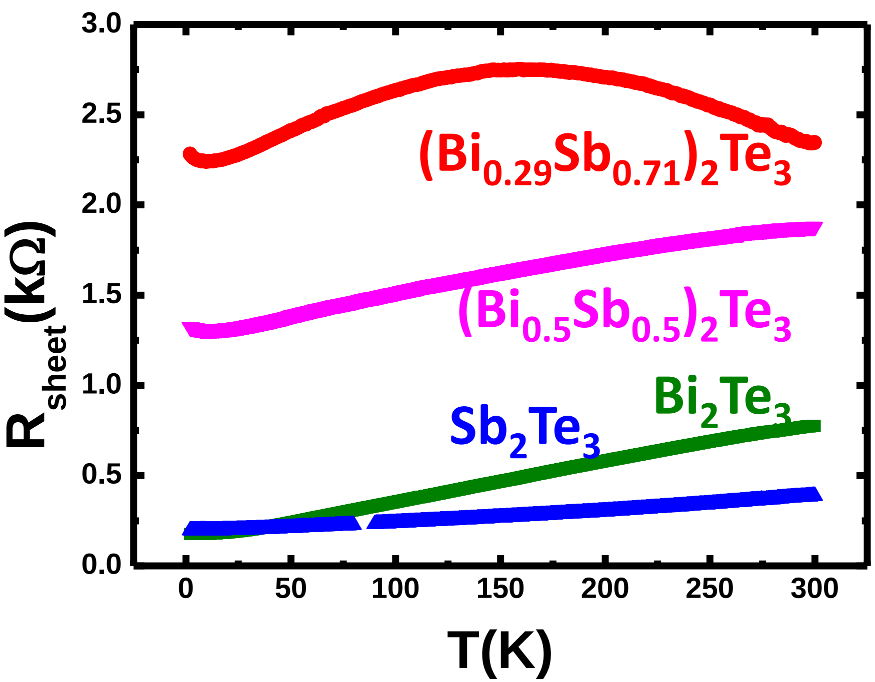

Semiconductor-like

- **Resistance increasing** with the temperature decreasing
- **Higher value** of resistance

Metal-like

- **Resistance decreasing** with the temperature decreasing

Te capping layer & R-T curves

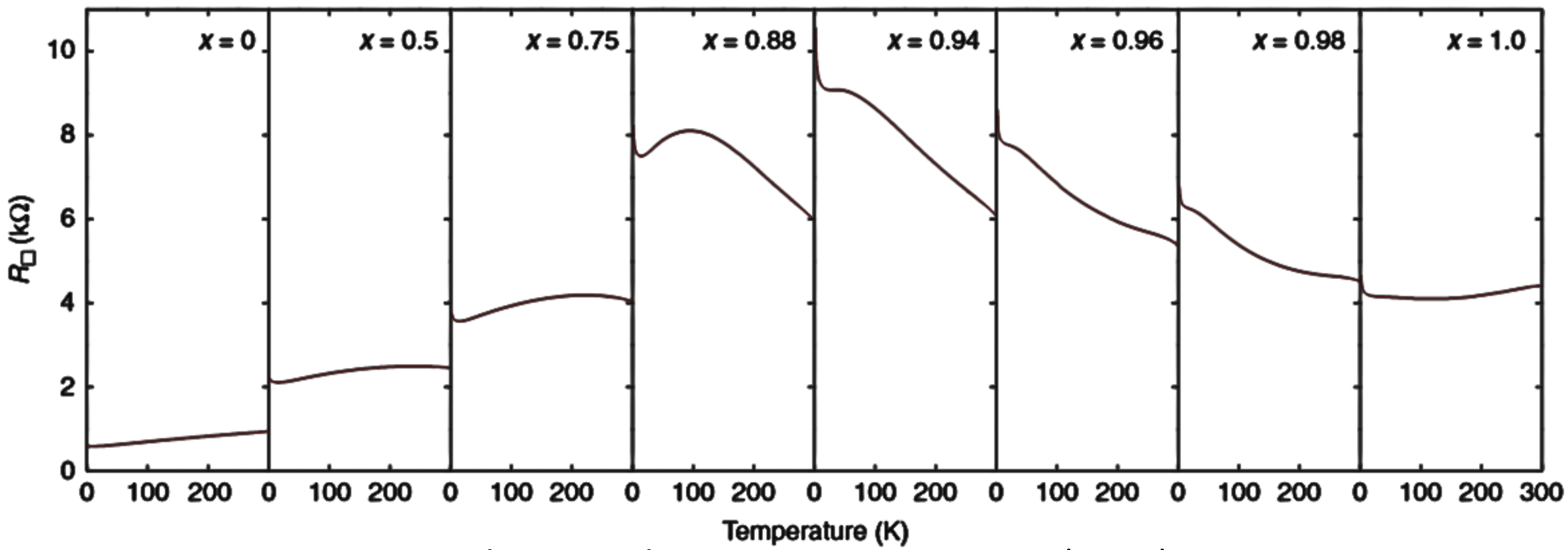

J. Zhang et al., Nat. Commun. **2**, 574 (2011).

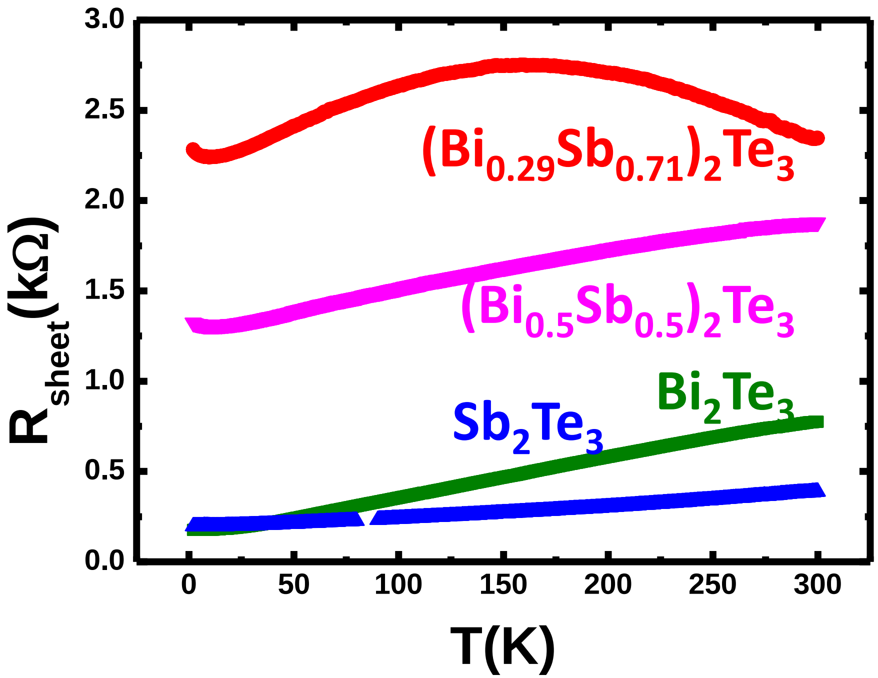

Semiconductor-like

- **Resistance increasing** with the temperature decreasing
- **Higher value** of resistance

Metal-like

- **Resistance decreasing** with the temperature decreasing

Te capping layer & R-T curves

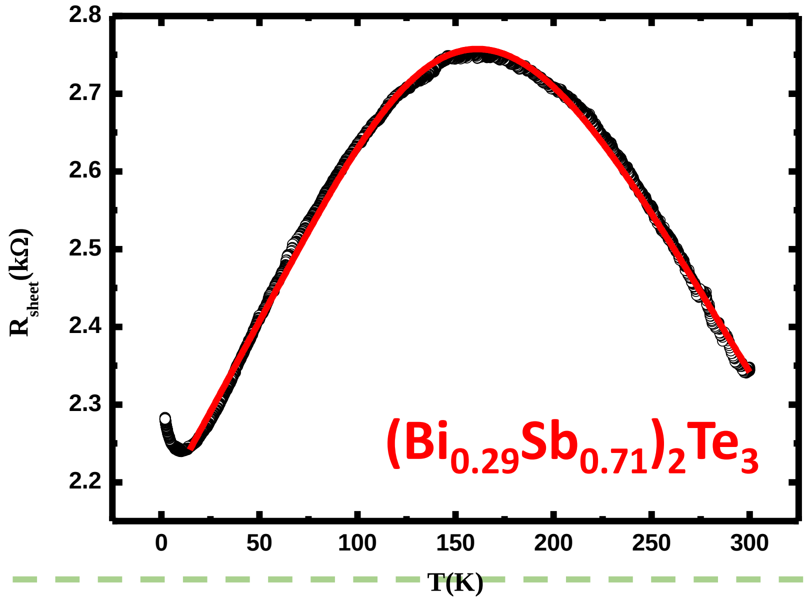

$$G_{total} = \frac{1}{R_0 + AT} + \frac{1}{R_1 \exp(\frac{\Delta}{kT})}$$

$R_0 = 2172\ \Omega$

$A = 4.7\ \Omega/T$

$R_1 = 701\ \Omega$

Δ=59 meV ⬅ activation energy

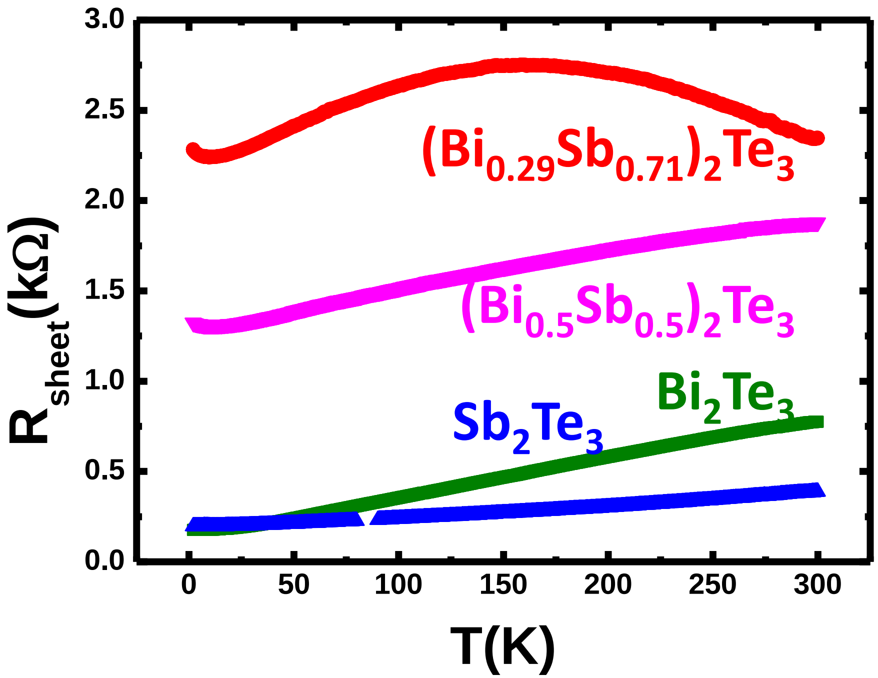

Semiconductor-like

- **Resistance increasing** with the temperature decreasing
- **Higher value** of resistance

Metal-like

- **Resistance decreasing** with the temperature decreasing

Te capping layer & R-T curves

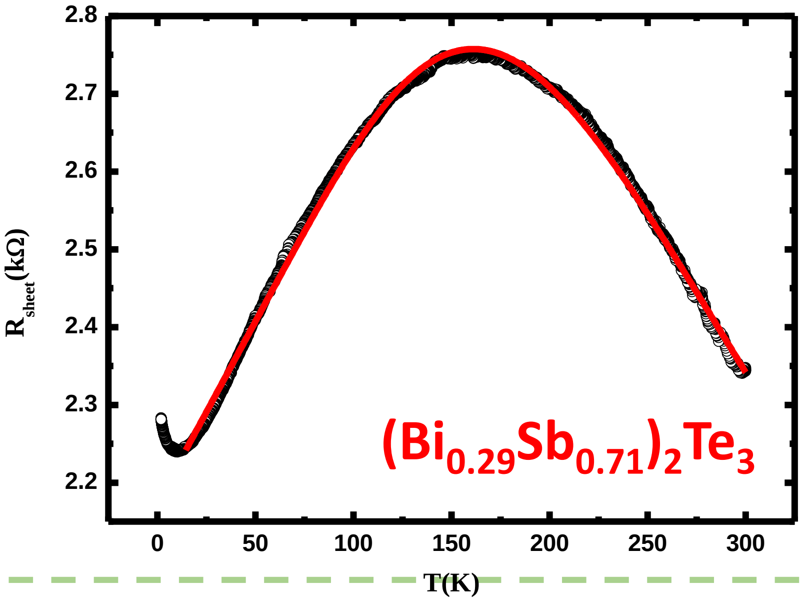

$$G_{total} = \frac{1}{R_0 + AT} + \frac{1}{R_1 \exp(\frac{\Delta}{kT})}$$

$R_0 = 2172\ \Omega$
$A = 4.7\ \Omega/T$
$R_1 = 701\ \Omega$
Δ=59 meV ⬅ activation energy

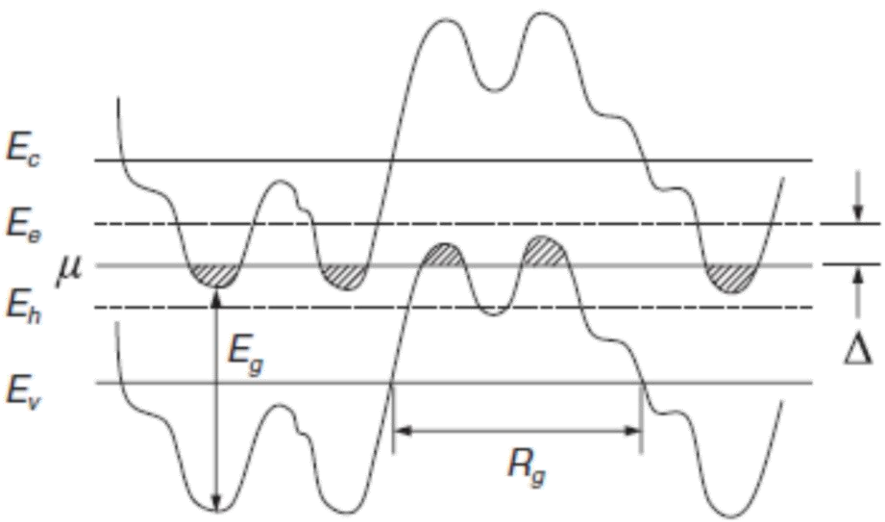

B. Skinner et al., Phys. Rev. Lett. **109**, 176801 (2012).

- **Network of p-n junction**
- **Activation energy ≈ energy from E_F to E_e (effective E_c)**
- **Larger Δ** of a TI **=>** **better quality**
- The **largest achievable Δ** of doped TI **is $0.15E_g \approx 50meV$** according to simulations.

Very low n_{2D} & boosted mobility

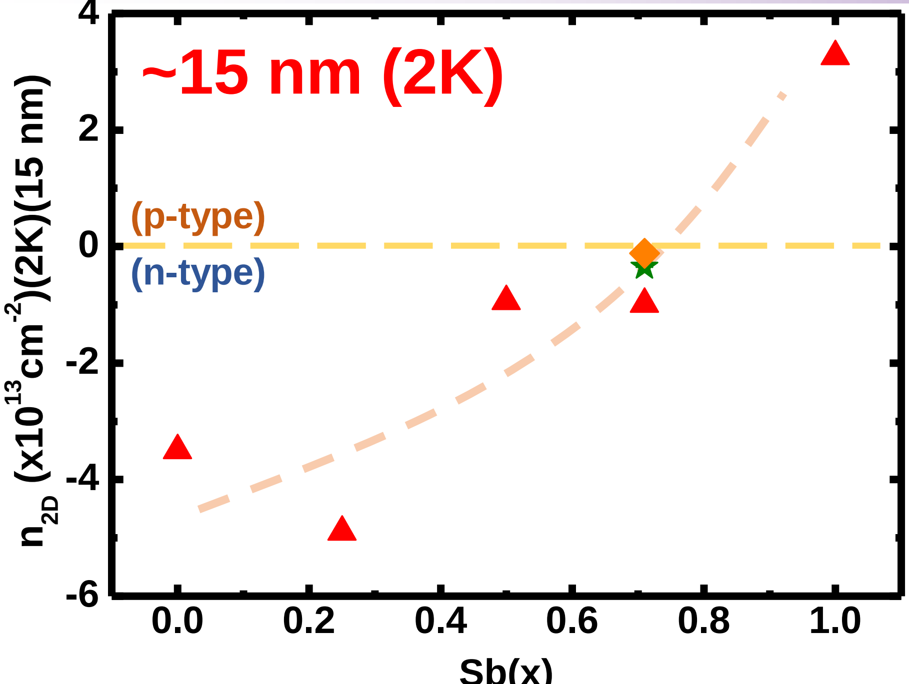

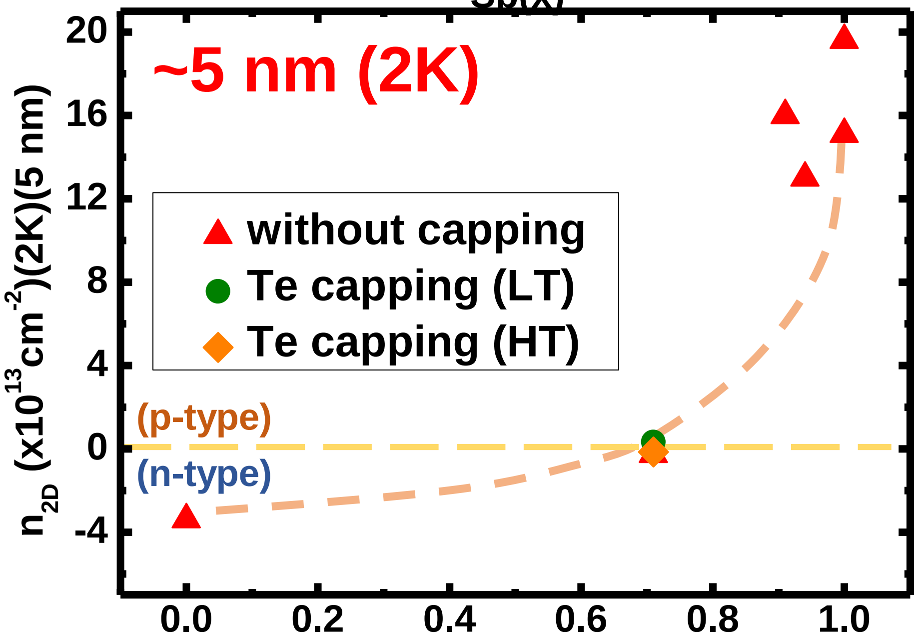

n_{2D}:

- Demonstration from **n-type to p-type**
- The lowest value of $-1.2 \times 10^{12}\ cm^{-2}$ **(15 nm)** and $-1.5 \times 10^{12}\ cm^{-2}$ **(5 nm)**

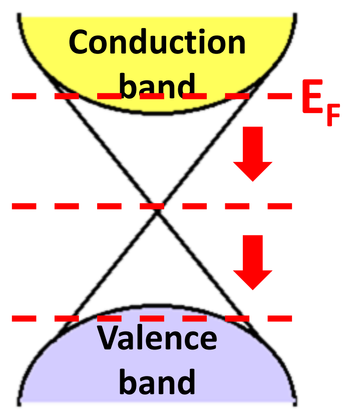

Very low n_{2D} & boosted mobility

Mobility:

- **Enhanced value** with capping layers
- Boosted value with **high-temp. growth**
- **Higher value** at Dirac point stemmed from the feature of **Dirac fermion**

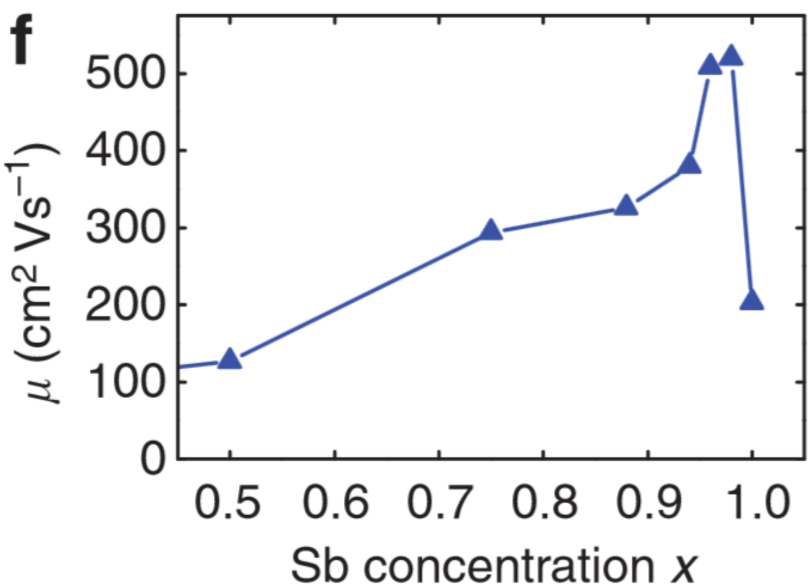

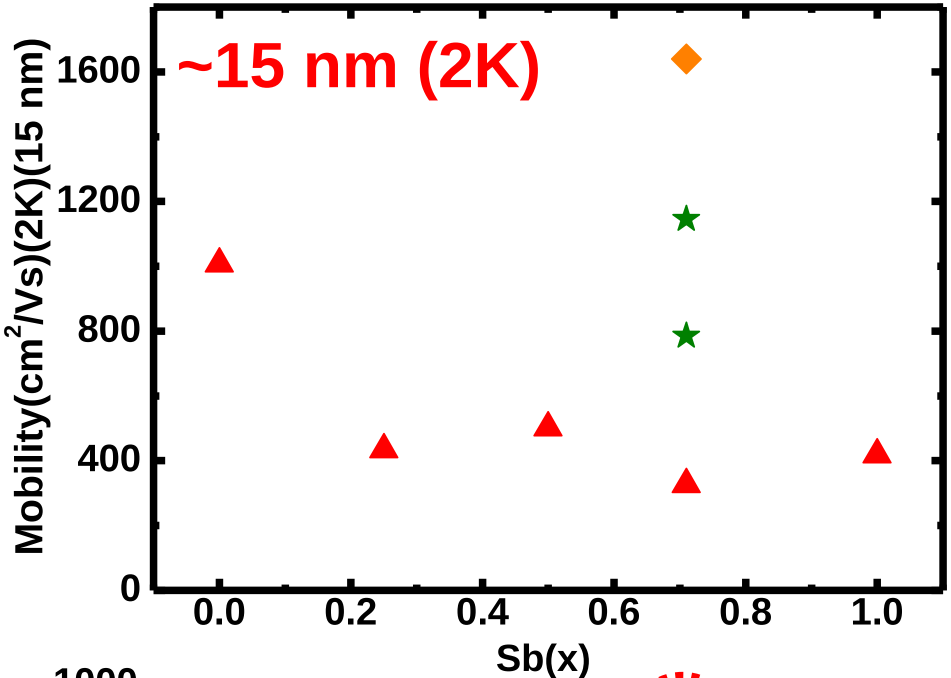

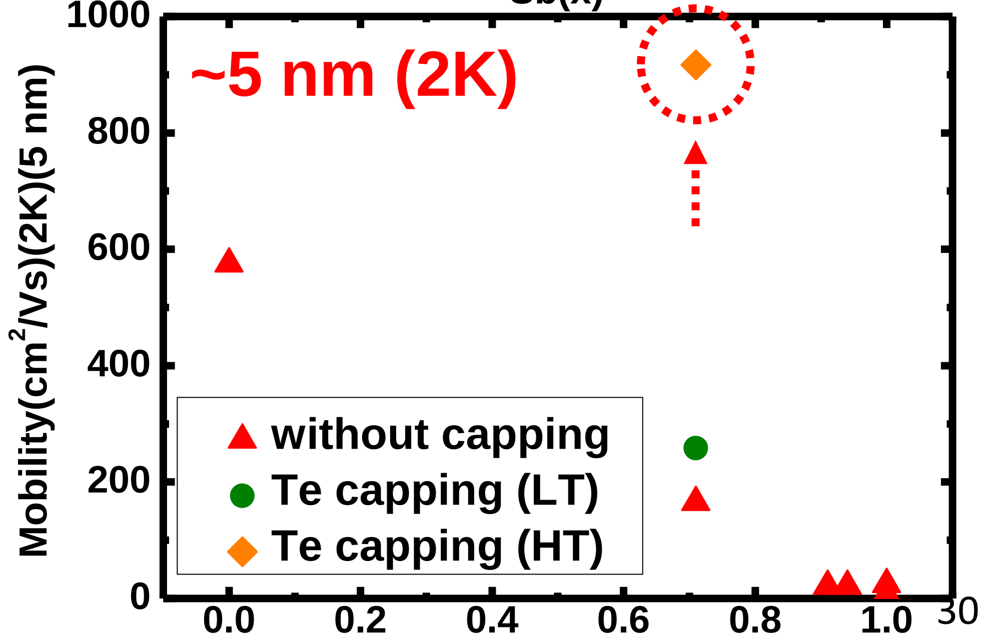

Two conductive transport channels

HLN equation:

$$\Delta G_{xx} = \alpha\left(\frac{e^2}{\pi h}\right)\left[\psi\left(\frac{\hbar}{4el^2B}+\frac{1}{2}\right)-\ln\left(\frac{\hbar}{4el^2B}\right)\right]+cB^2$$

$\alpha \sim -0.5$: one channel with weak anti-localization (WAL)

$\alpha \sim -1$: two channel with WAL

***l*: phase coherence length**

(1) the **Sb composition** dependence

(2) the effect of the **capping layer**

(3) the **BST thickness** dependence

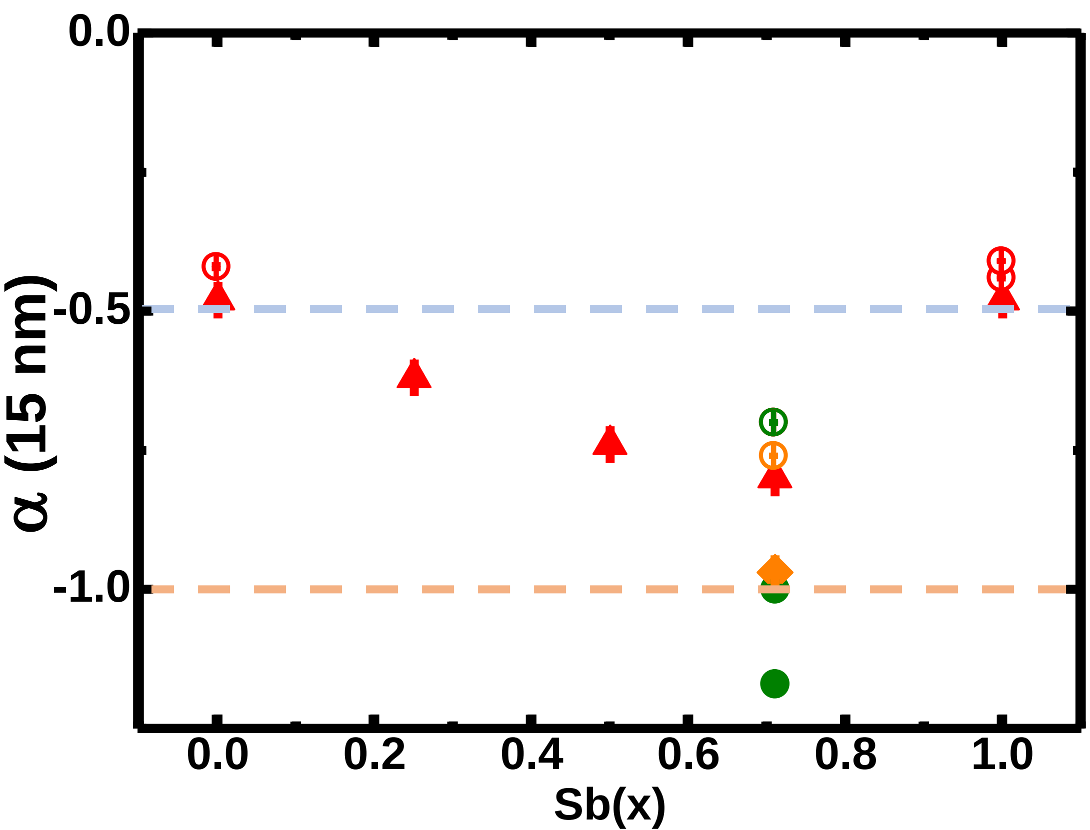

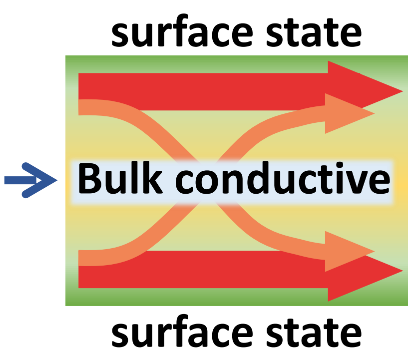

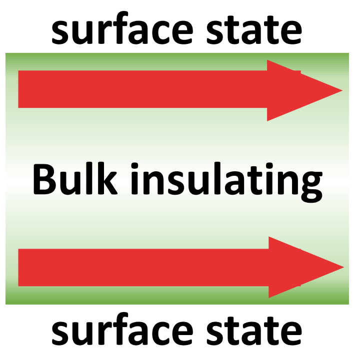

Two conductive transport channels

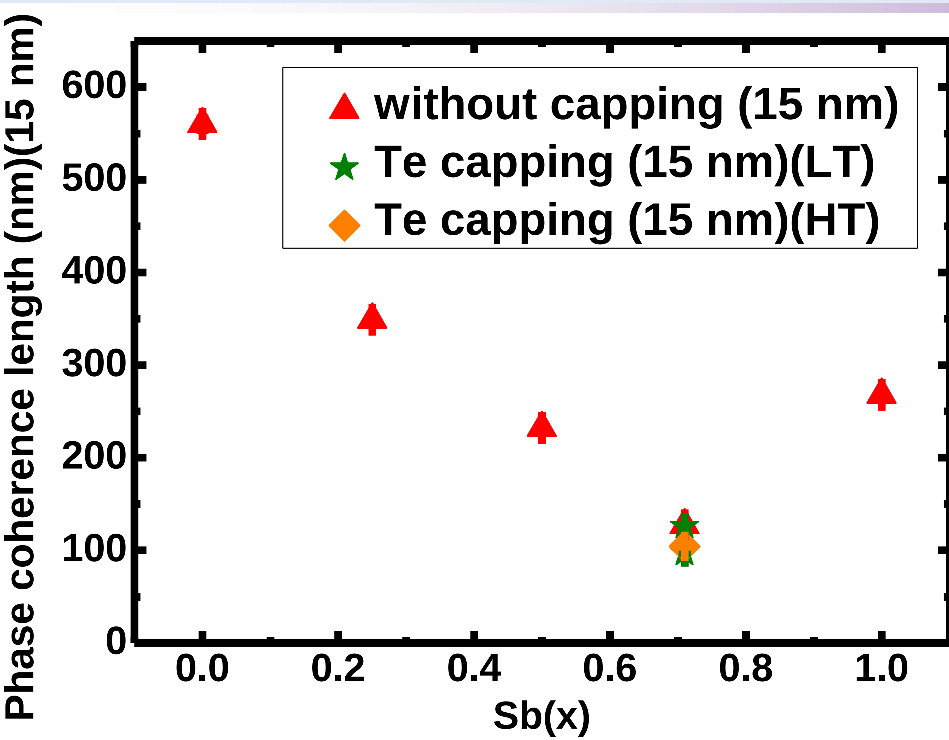

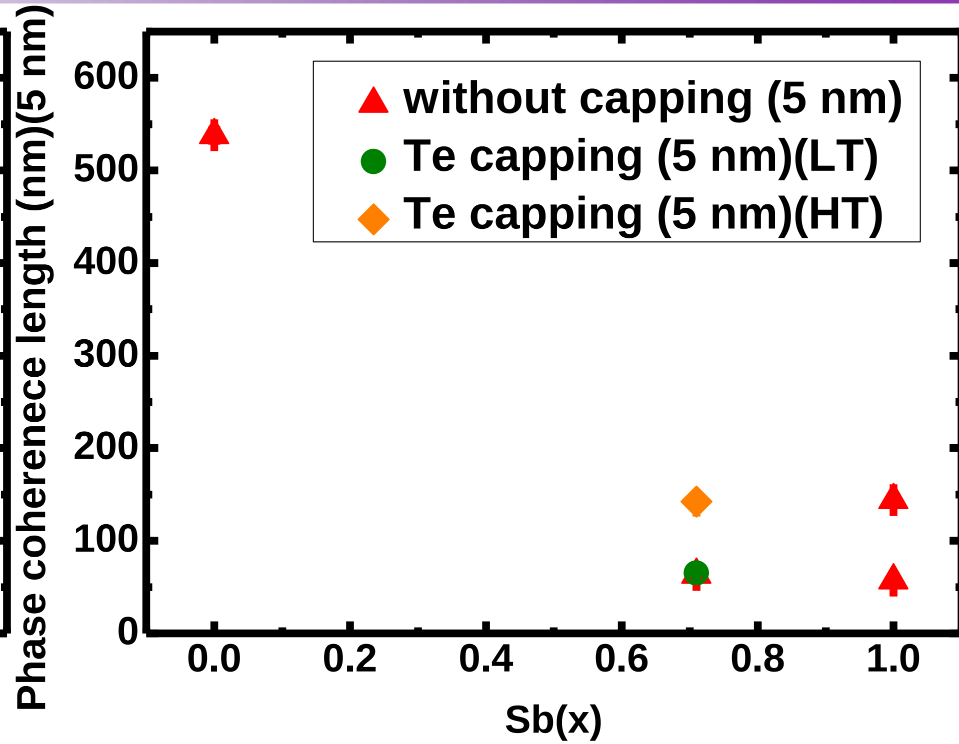

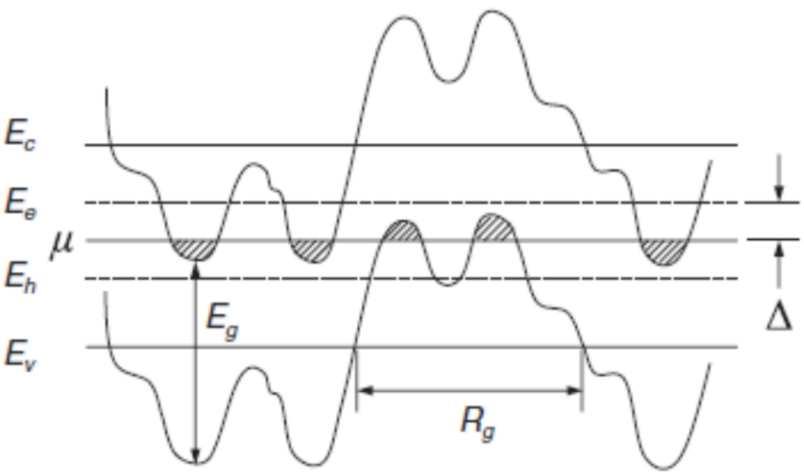

B. Skinner et al., Phys. Rev. Lett. **109**, 176801 (2012).

Low phase coherence length of $(Bi,Sb)_2Te_3$

- **Network of p-n junction**
- Transport by means of **hopping** or **tunneling between charge puddles**
- **Enhanced coherence length with the high-temperature growth**

Tuning E_F and band structures

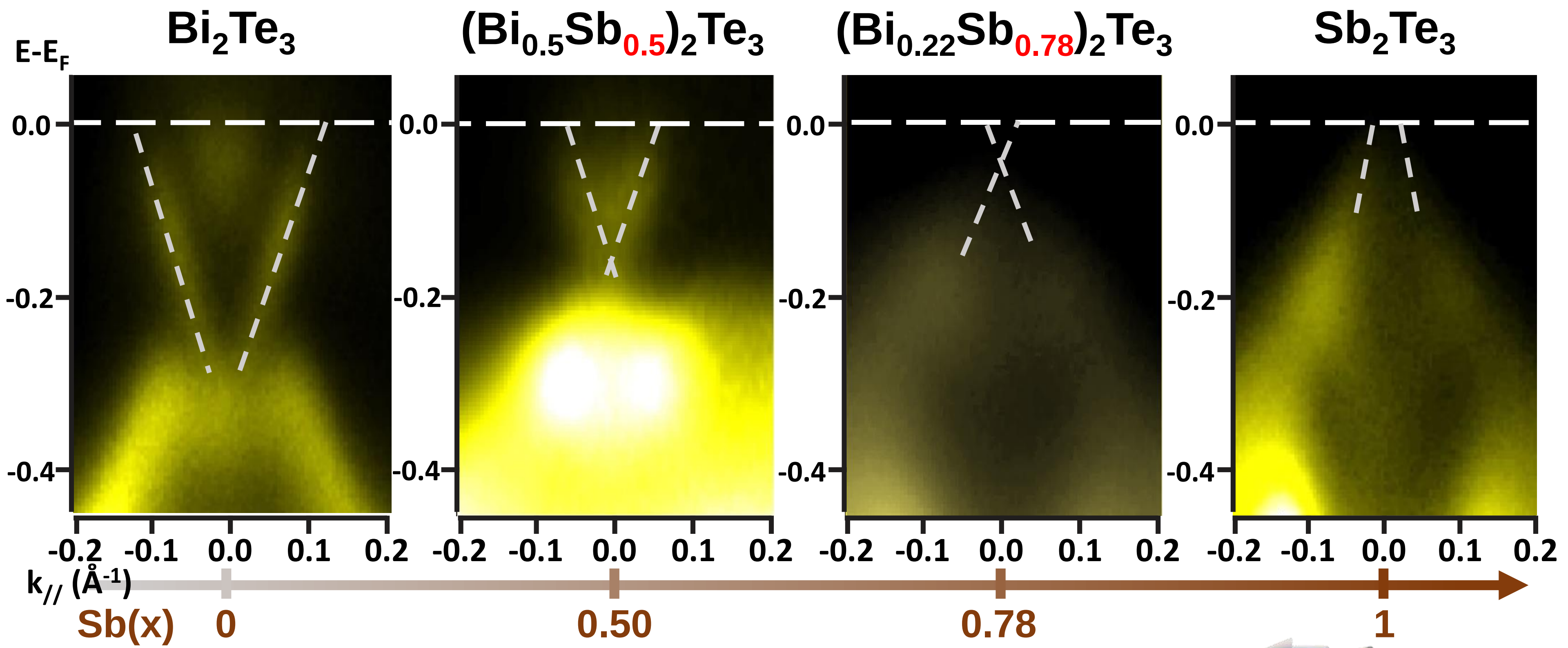

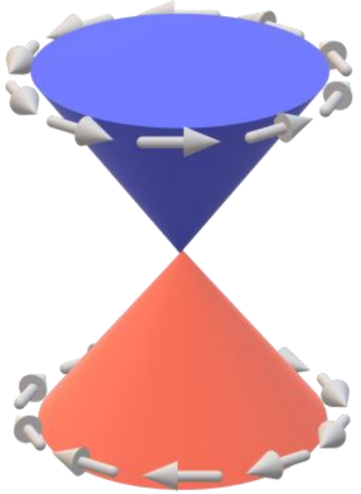

- **Tuning E_F** across the Dirac point
- **Clear surface states** shown in all samples

Condition:

- **He I hv = 21.2 eV**
- **At 300K**
- **Thickness = ~20 nm**
- **K− Γ− K**

Modified SBLT growth (Te-based TI)

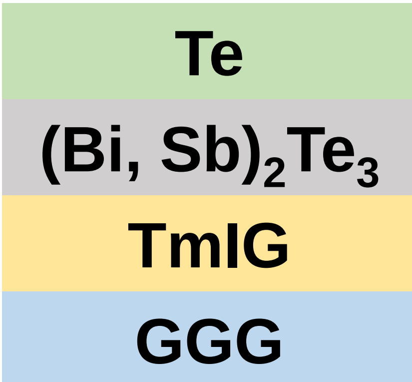

Breaking TRS by **MPE**

Low-temperature growth

(modified from **Se-buffered low-temp. (SBLT) growth**)

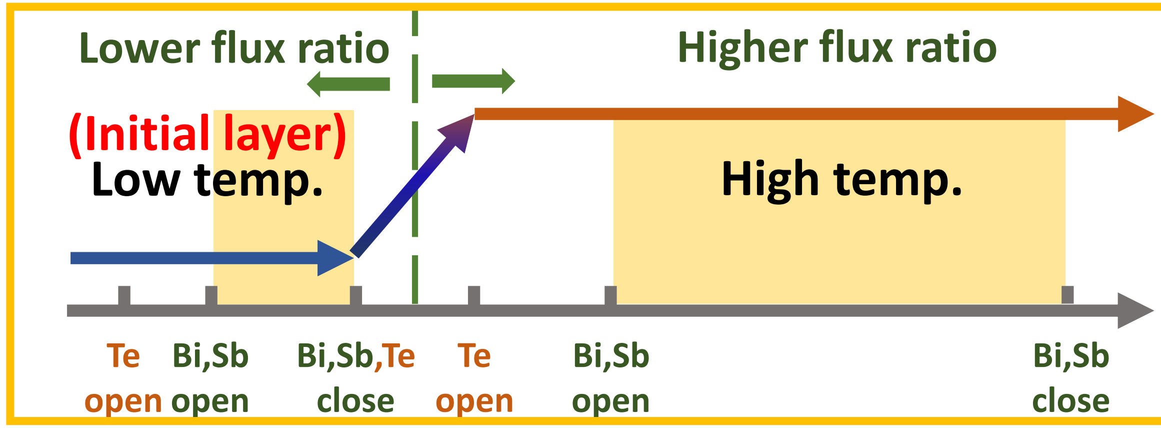

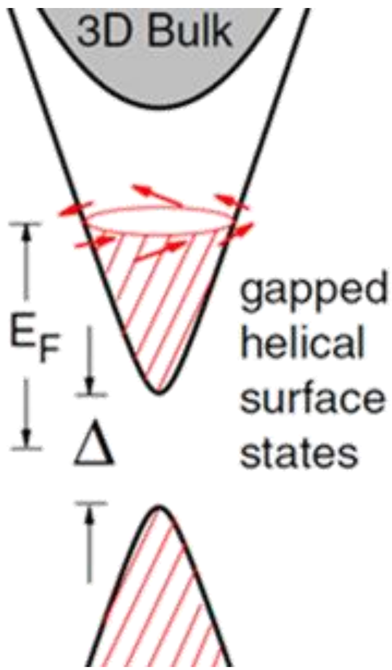

H.-Z. Lu *et al.*, PRL **107**, 076801 (2011).

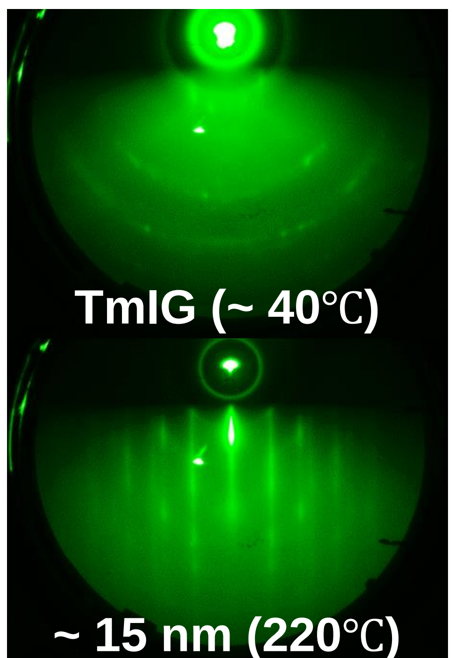

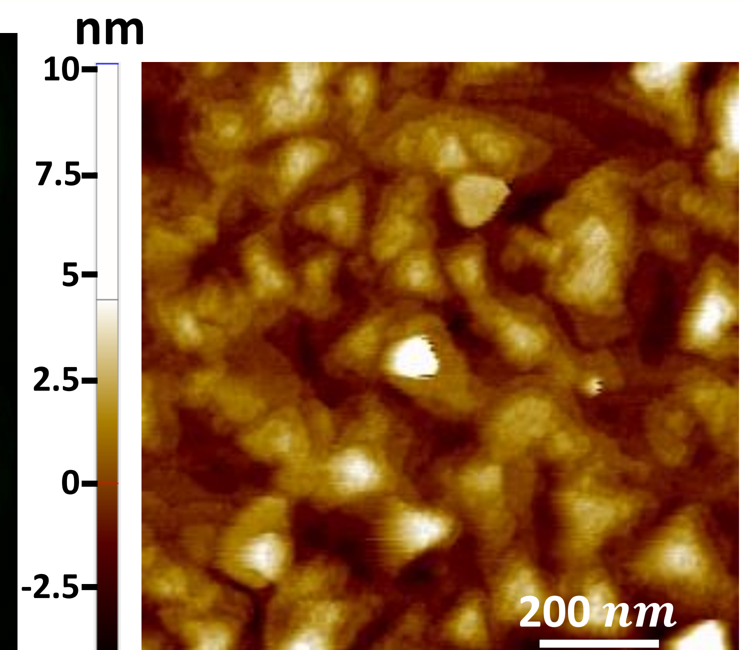

Roughness = 1.42 nm

Observation of AHE up to RT

~ one order larger R_{AHE} than that in Bi_2Se_3/TmIG

$(Bi,Sb)_2Te_3$/TmIG (in this work) **Bi_2Se_3/TmIG (our previous work)**

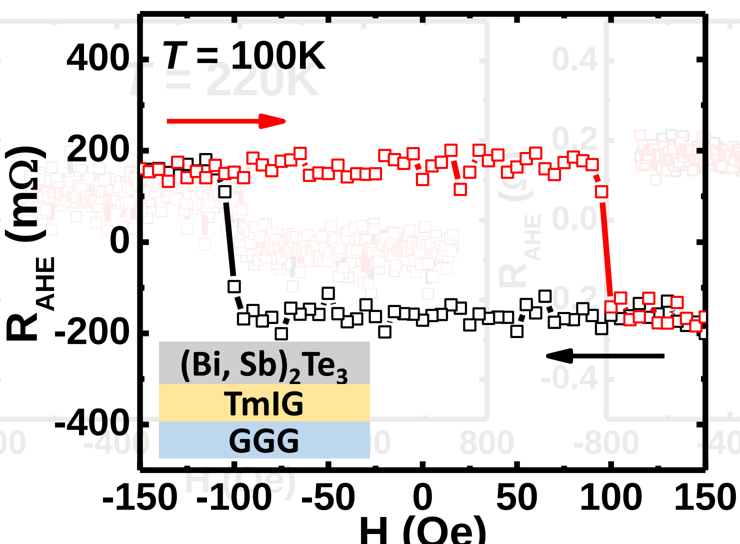

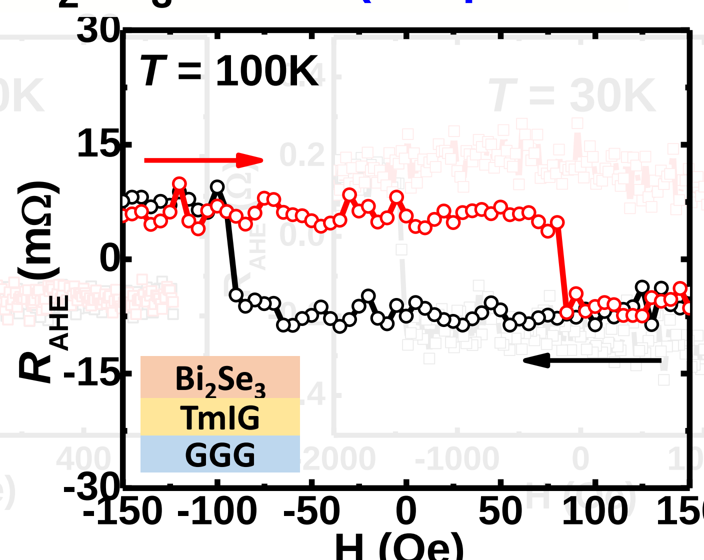

Observation of AHE up to RT

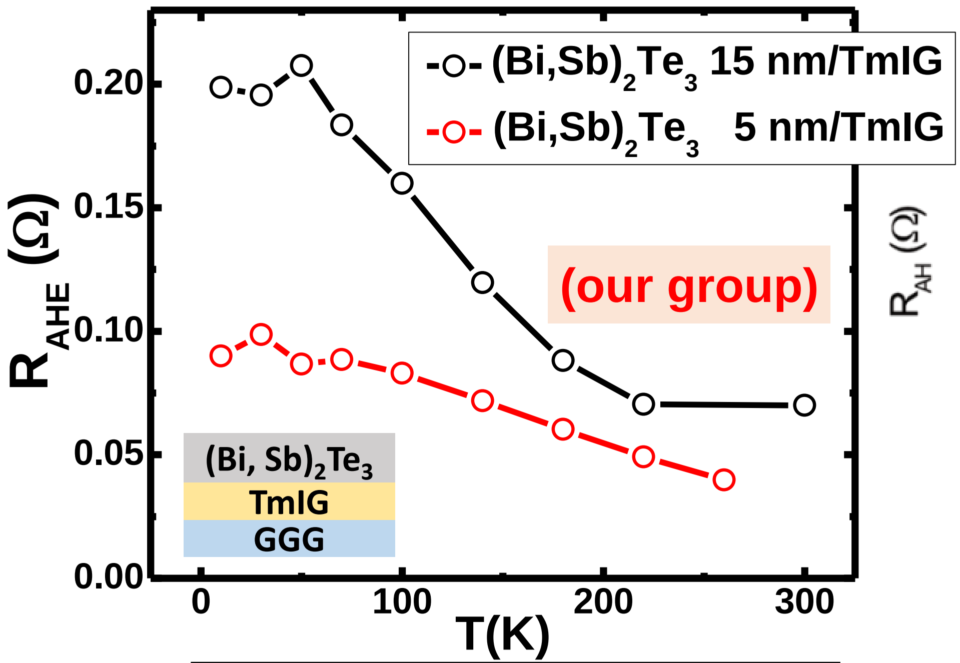

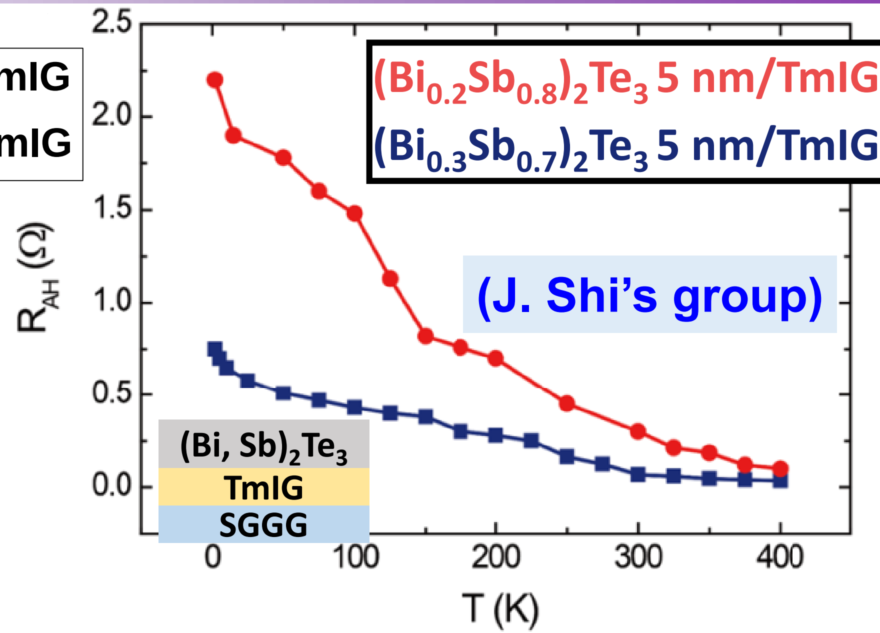

C. Tang *et al.*, Sci. Adv. **3** (6), e1700307 (2017).

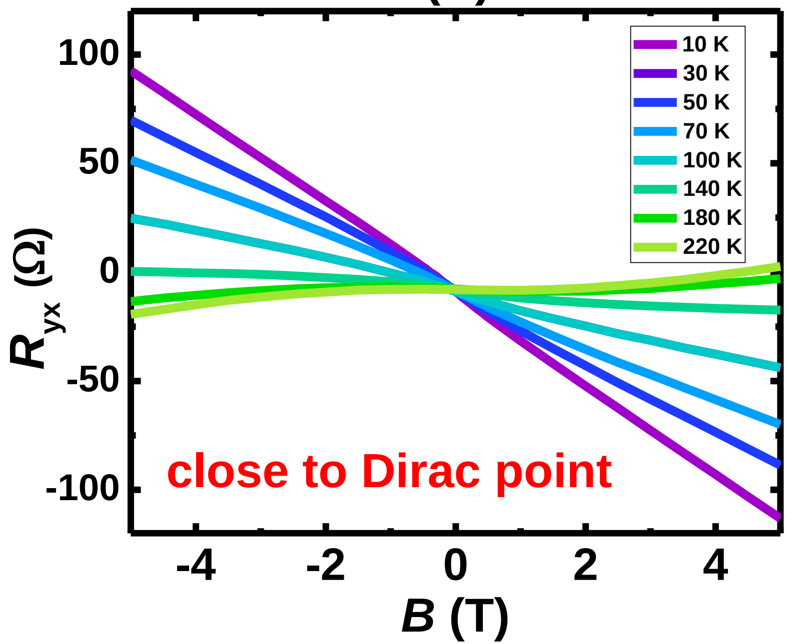

Factors affect the extent of R_{AH}:

- **Stronger PMA induced by SGGG**
  - **Larger tensile strain**
- **E_F closer to Dirac point**

  M. Li *et al.*, Phys. Rev. B **96**, 201301(R) (2017).
- **Interface quality**

R-T curves of $(Bi,Sb)_2Te_3$/TmIG

R-T curve

~ 15 nm

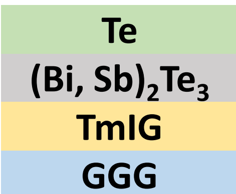

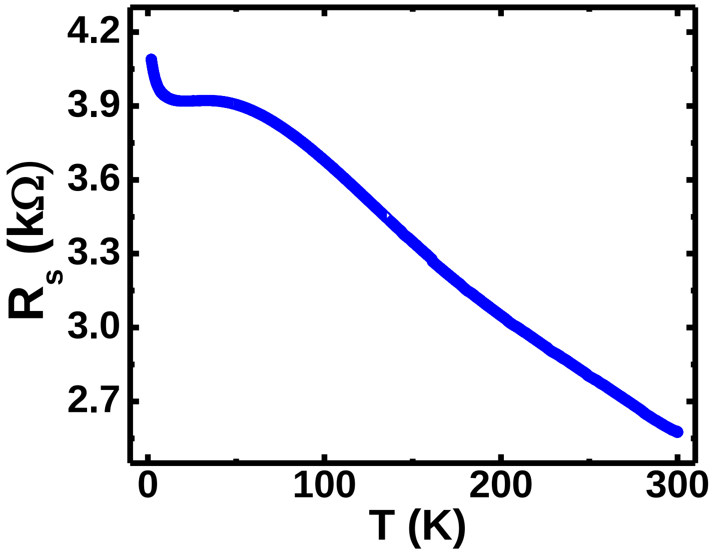

~ 5 nm

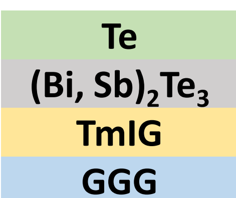

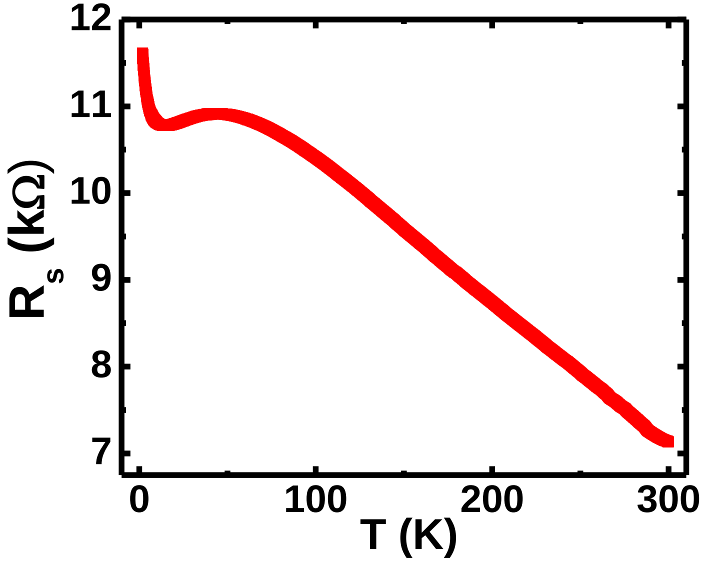

- **Semiconductor-like feature in** both samples
- Similar to the previous work

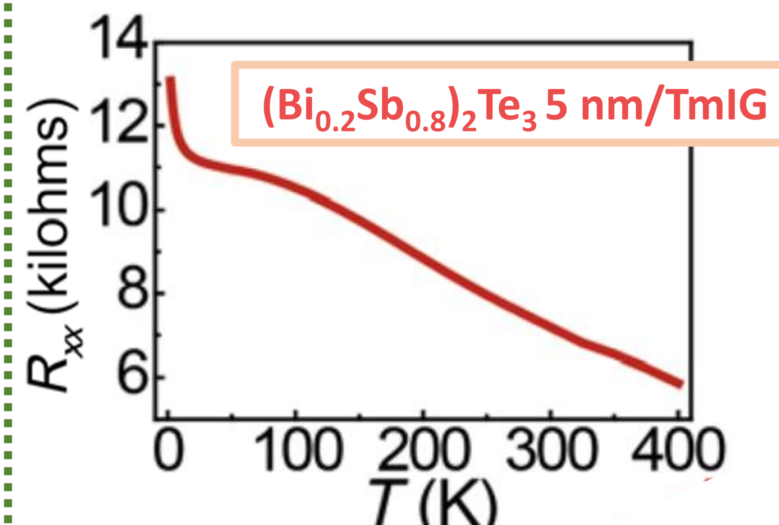

C. Tang *et al.*, Sci. Adv. **3** (6), e1700307 (2017).

MR analysis by HLN equation

MR

~ 15 nm

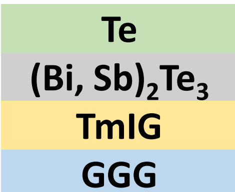

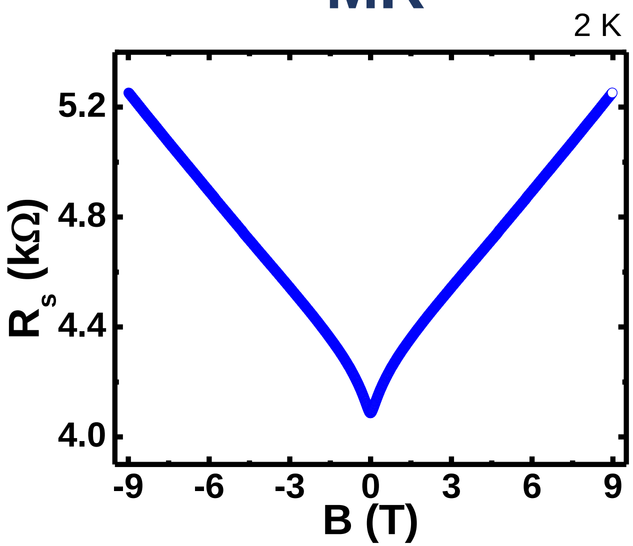

~ 5 nm

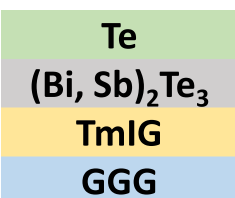

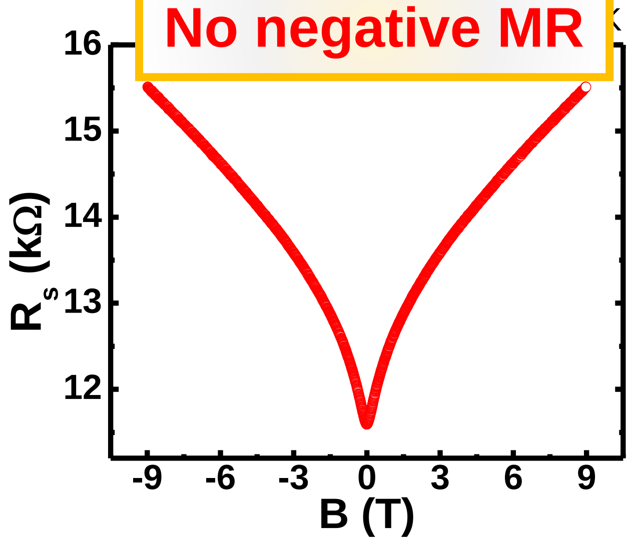

No negative MR

Bi_2Se_3/TmIG (our work)

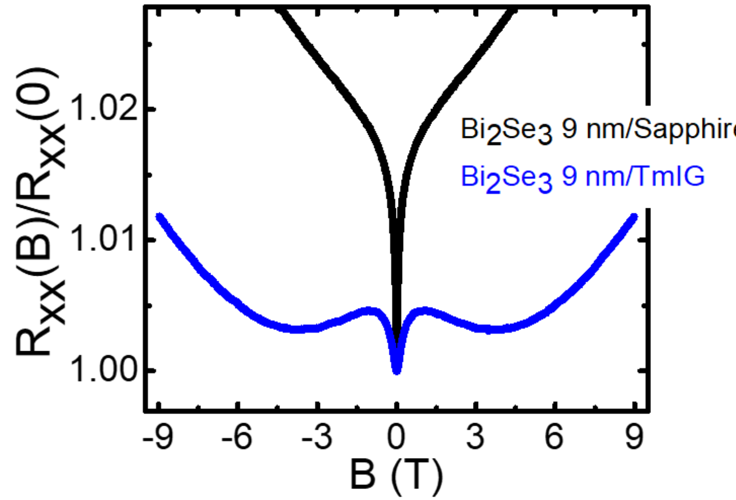

S. R. Yang et al., arXiv: 1811.00689 (2018).

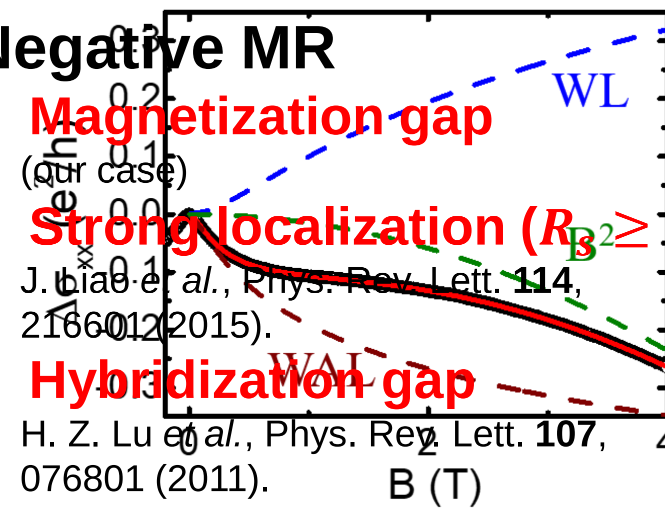

Negative MR

- **Magnetization gap** (our case)
- **Strong localization ($R_s \geq h/e^2$)**
  J. Liao *et al.*, Phys. Rev. Lett. **114**, 216601 (2015).
- **Hybridization gap**
  H. Z. Lu *et al.*, Phys. Rev. Lett. **107**, 076801 (2011).

MR analysis by HLN equation

- **No negative MR**
- **Suppressed WAL**
- **Smaller magnitude of α in $(Bi,Sb)_2Te_3$/TmIG** than those on Sapphire

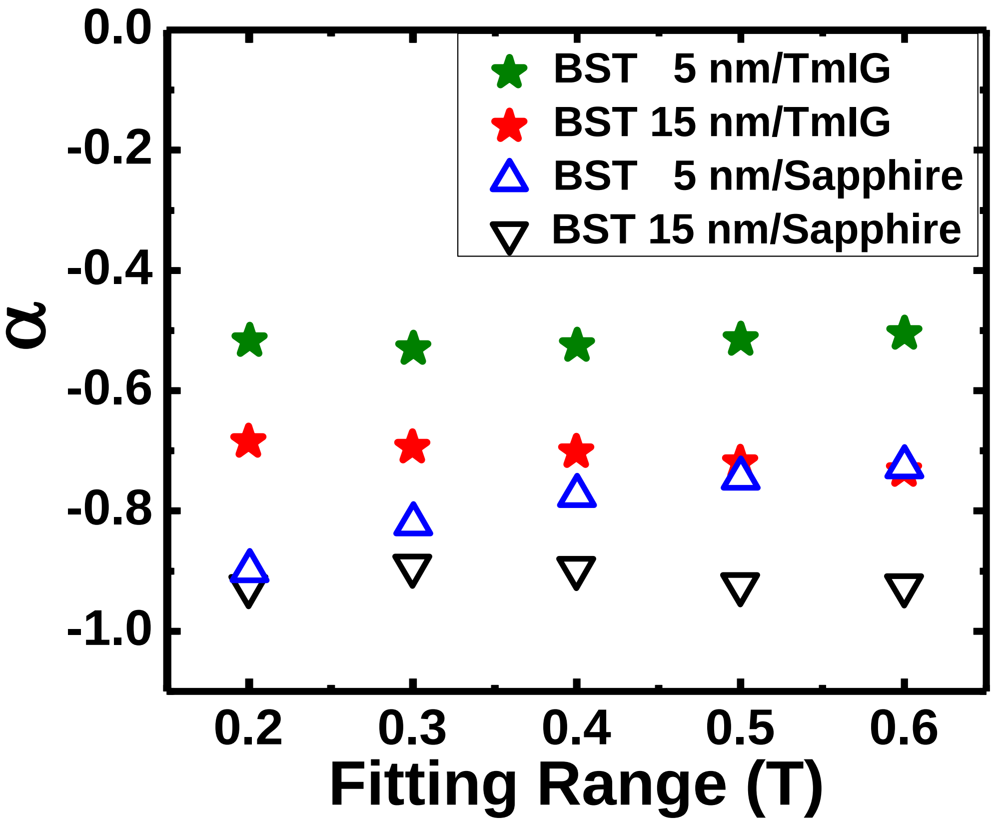

Bi_2Se_3/TmIG (our work)

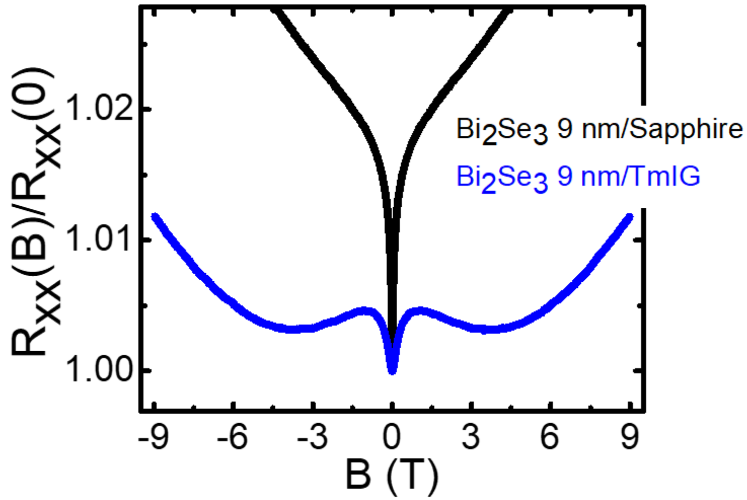

$(Bi,Sb)_2Te_3$/TmIG (this work)

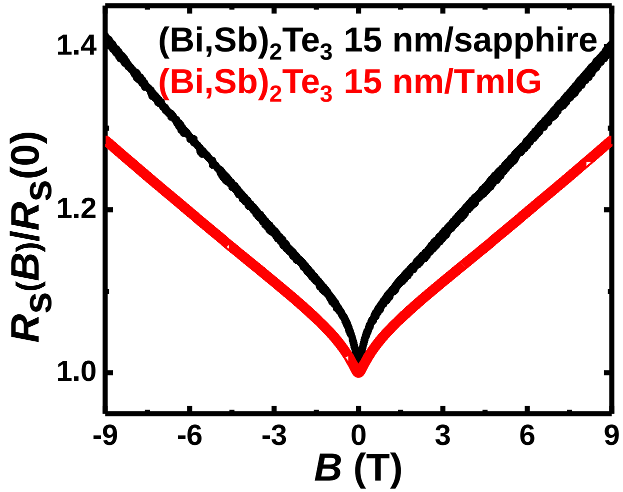

MR analysis by HLN equation

When the top surface and the bottom surface are decoupled,

$\Delta\sigma_{total} = \sigma_{top\ surface} + \sigma_{bottom\ surface}$

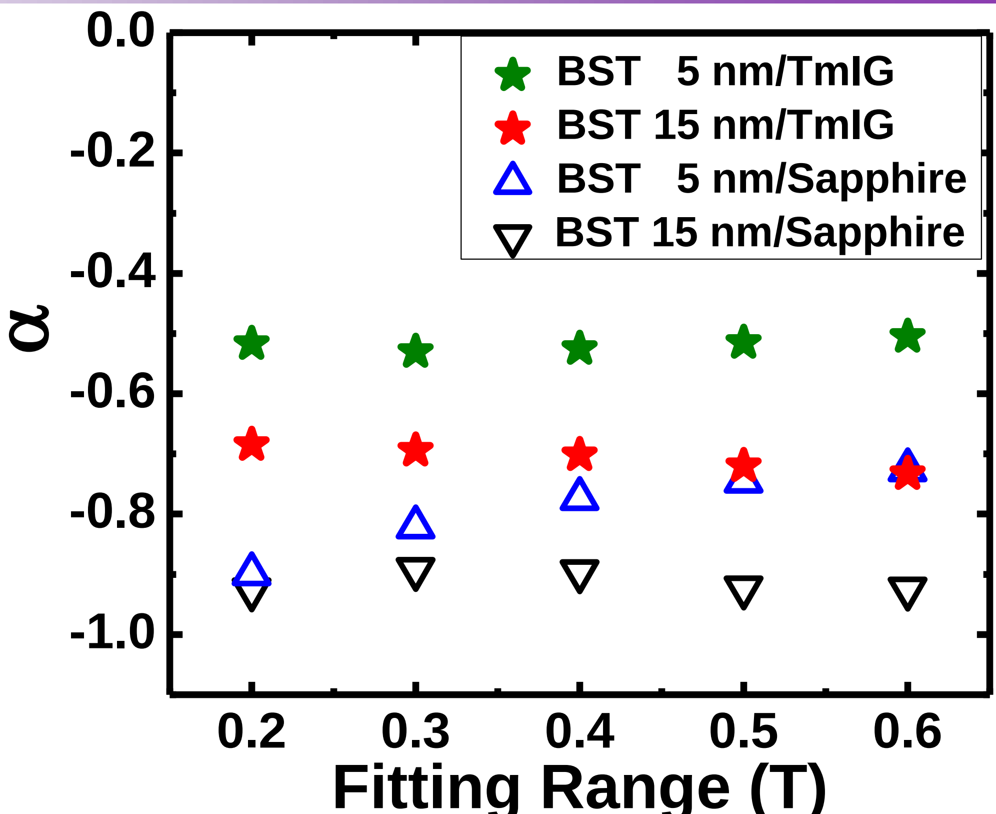

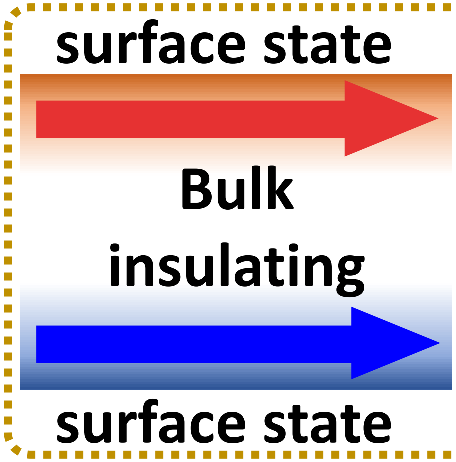

➡ $\sigma_{top\ surface} = \mathbf{WAL}\ (\alpha = -0.5)$

➡ $\sigma_{bottom\ surface} = \mathbf{WAL}\ (-0.5 < \alpha < 0) + \mathbf{WL}\ (0 < \alpha < 0.5)$

Summary II

Excellent crystallinity in $(Bi,Sb)_2Te_3$ on **α-Al_2O_3**

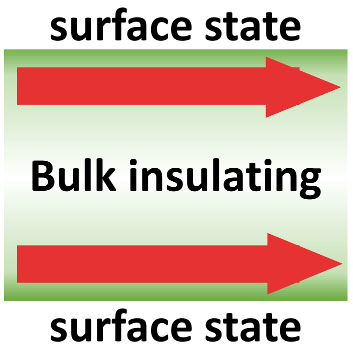

- Transport: **lowest n_{2D}, two conducting channels**
- ARPES: closer to **Dirac point**

Excellent crystallinity in $(Bi,Sb)_2Te_3$ on **TmIG**

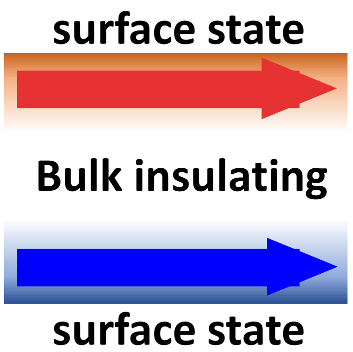

- **Room-temperature AHE**
- Weak thickness dependence ➡ **insulating bulk**
- **No negative MR** with smaller magnitude of α

➡ **MPE only affected the bottom surface**

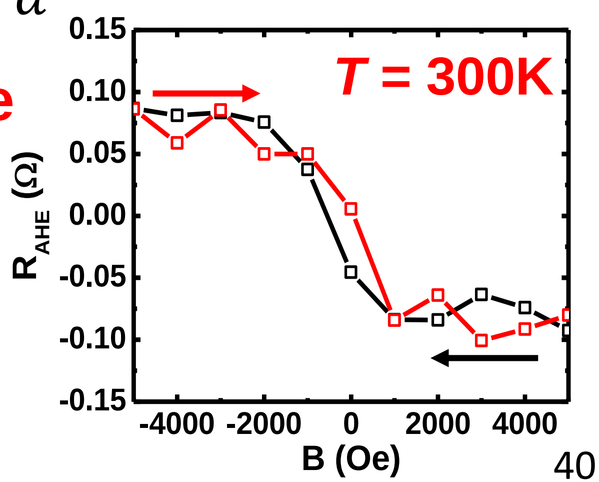

Conclusion

Conclusion

Bi_2Se_3 / **ReIG**	• **Breaking time reversal symmetry** • Improvement of the **interface quality** • Enhancement of the **interfacial exchange coupling**
$(Bi,Sb)_2Te_3$ / **α-Al_2O_3**	• **Toward insulating bulk state** • Two conductive transport channels • Band engineering revealed by ARPES
$(Bi,Sb)_2Te_3$ / **TmIG**	• Modifying the growth from Bi_2Se_3/ReIG • Pushing the **T_C up to room temperature** (AHE)